HHS Public Access

Author manuscript

Mol Microbiol. Author manuscript; available in PMC 2018 April 01.

Published in final edited form as:

Mol Microbiol. 2017 April ; 104(1): 105–124. doi:10.1111/mmi.13616.

Analysis of [*SWI*$^{+}$] Formation and Propagation Events

Zhiqiang Du[*], **Dustin Kenneth Goncharoff**, **Xudong Cheng**, and **Liming Li**[*]

Department of Biochemistry and Molecular Genetics, the Feinberg School of Medicine, Northwestern University. 320 E Superior St, Searle 7-650, Chicago IL 60611.

Summary

The budding yeast, *Saccharomyces cerevisiae,* harbors several prions that are transmitted as altered, heritable protein conformations. [*SWI*$^{+}$] is one such prion whose determinant is Swi1, a subunit of the evolutionarily conserved chromatin-remodeling complex SWI/SNF. Despite the importance of Swi1, the molecular events that lead to [*SWI*$^{+}$] prionogenesis remain poorly understood. In this study, we have constructed floccullin-promoter-based *URA3* reporters for [*SWI*$^{+}$] identification. Using these reporters, we show that the spontaneous formation frequency of [*SWI*$^{+}$] is significantly higher than that of [*PSI*$^{+}$] (prion form of Sup35). We also show that preexisting [*PSI*$^{+}$] or [*PIN*$^{+}$] (prion form of Rnq1), or overproduction of Swi1 prion-domain (PrD) can considerably promote Swi1 prionogenesis. Moreover, our data suggest a strain-specific effect of overproduction of Sse1 – a nucleotide exchange factor of the molecular chaperone Hsp70, and its interaction with another molecular chaperone Hsp104 on [*SWI*$^{+}$] maintenance. Additionally, we show that Swi1 aggregates are initially ring/ribbon-like then become dot-like in mature [*SWI*$^{+}$] cells. In the presence of [*PSI*$^{+}$] or [*PIN*$^{+}$], Swi1 ring/ribbon-like aggregates predominantly colocalize with the Sup35 or Rnq1 aggregates; without a preexisting prion, however, such colocalizations are rarely seen during Swi1-PrD overproduction-promoted Swi1 prionogenesis. We have thus demonstrated a complex interacting mechanism of yeast prionogenesis.

Graphical abstract

[*]Correspondence: Liming Li, limingli@northwestern.edu, 1-312-503-4420, Zhiqiang Du, z-du@northwestern.edu, 1-312-503-4421 .

Supplemental information

Three tables and five figures are included

Author Contributions

ZD, LL initiated the project and designed the experiments. ZD performed most of the experiments. DKG performed part of [*SWI*$^{+}$] de novo formation experiments. XC conducted part of the [*SWI*$^{+}$] propagation experiments. ZD and LL analyzed data. ZD, DKG, and LL wrote the manuscript.

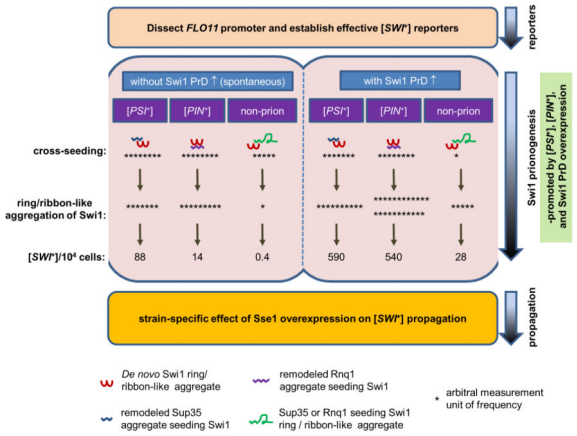

We have dissected the yeast *FLO11* promoter and constructed several truncated *FLO11*-promoter-based reporters for studying the events of [*SWI*$^+$] *de novo* formation and propagation. We show that in the presence of [*PSI*$^+$] or [*PIN*$^+$], cross-seeding with Sup35 or Rnq1 is a prevalent mechanism promoting Swi1 aggregation and prionogenesis, but not when [*SWI*$^+$] formation is merely promoted by Swi1 prion-domain overproduction. We also show a strain-specific sensitivity of [*SWI*$^+$] to overproduction of the molecular chaperone Sse1.

Keywords

prion; Swi1; SWI/SNF; aggregation; prion-interactions

Introduction

Prions, proteinaceous infectious particles, are composed of host proteins with altered and transmissible conformations (Wickner *et al.*, 2015, Colby & Prusiner, 2011). Although the term prion was first used to describe the causative agent of the neurodegenerative diseases known as transmissible spongiform encephalopathies (TSEs) (Prusiner, 1982, Prusiner, 1998), this protein-only prion concept has been expanded to include a large number of fungal and mammalian proteins that can also undergo conformational changes and be transmitted as highly-ordered aggregates termed amyloids (Crow & Li, 2011, Munch *et al.*, 2011, Sanders *et al.*, 2014, Luk *et al.*, 2012). In the budding yeast *Saccharomyces cerevisiae*, at least nine prion proteins have been identified and additional potential prions may exist (Crow & Li, 2011, Suzuki *et al.*, 2012, Halfmann *et al.*, 2012, Chakrabortee *et al.*, 2016). When these prion proteins adopt prion conformation(s), the resulting prions usually manifest as dominant and heritable features, mostly through modulation of important cellular processes such as transcription and translation (Alberti *et al.*, 2009, Du *et al.*, 2015, Serio & Lindquist, 1999, Stein & True, 2014). In addition, it has been shown that some yeast prions can exist in wild strains and their prion conformational switches can be environmentally responsive, suggesting a possible role of prionogenesis in yeast adaptation to environmental fluctuations (Holmes *et al.*, 2013, Suzuki *et al.*, 2012, Jarosz *et al.*, 2014, Tyedmers *et al.*, 2008). Interestingly, protein misfolding, aggregation, and subsequent amyloid deposition have been proposed to be crucial etiological events associated with more than 40 incurable

mammalian disorders, including Alzheimer's disease (AD), Parkinson's disease (PD), Huntington's disease (HD), and amyotrophic lateral sclerosis (ALS) and recently, cancers (Ano Bom *et al.*, 2012, Luk *et al.*, 2012, Munch *et al.*, 2011, Sanders *et al.*, 2014).

Amyloid yeast prions have become valuable systems for studying prion biology and other proteinopathies due to sharing similar structural features and transmission mechanisms as PrP^{Sc}, the causative agent of TSEs, and several other prion-like mammalian pathogenic proteins, such as tau (a microtubule-associated protein implicated in tauopathies when misfolded (Alonso *et al.*, 2001)), β-amyloid (peptides of 36–43 amino acids derived from a protein known as amyloid protein precursor and implicated in Alzheimer's disease (Vassar *et al.*, 1999), and α-synuclein (an abundant protein in the brain implicated in a group of disorders known as synucleinopathies when it becomes insoluble (Spillantini *et al.*, 1997)) . Utilizing the yeast prion systems, important knowledge has been gained regarding molecular mechanisms of prion formation and transmission and important cellular factors required for prionogenesis, such as molecular chaperones – Hsp104, Hsp40, and Hsp70 and its co-chaperones – have been identified (see reviews of (Guinan & Jones, 2009, Romanova & Chernoff, 2009, Winkler *et al.*, 2012, Sporn & Hines, 2015)). In addition, valuable information regarding how heterologous prion proteins interact with each other and how such interactions influence their *de novo* prion formation and maintenance has also been reported (Derkatch *et al.*, 2001, Derkatch *et al.*, 1997, Du & Li, 2014, Osherovich & Weissman, 2001, Schwimmer & Masison, 2002).

Perhaps the most studied yeast prion is [*PSI*$^{+}$], whose protein determinant is Sup35, a translational termination factor (Stansfield *et al.*, 1995). When Sup35 enters a prion conformation, it results in a compromised translation termination function (Patino *et al.*, 1996). Previously, it was reported that overproduction of Swi1, a subunit of the SWI/SNF chromatin-remodeling complex, can facilitate *de novo* formation of [*PSI*$^{+}$] (Derkatch *et al.*, 2001). We later reported that Swi1 can exist as a prion, [*SWI*$^{+}$], and cells harboring [*SWI*$^{+}$] exhibit a partial loss-of-function phenotype of SWI/SNF (Du *et al.*, 2008). We also showed that preexisting [*SWI*$^{+}$] can promote the *de novo* formation of [*PSI*$^{+}$] and another prion known as [*PIN*$^{+}$] or [*RNQ*$^{+}$], whose protein determinant is Rnq1 (Du & Li, 2014, Sondheimer & Lindquist, 2000, Derkatch *et al.*, 1997). Such [*PSI*$^{+}$] or [*PIN*$^{+}$] promotion by [*SWI*$^{+}$] is likely realized mainly through a cross-seeding mechanism. The cross-seeding model proposes that a preexisting prion can provide a conformational template on which the first seeds of a different prion can form (Derkatch *et al.*, 2001). In this case, the Swi1 prion aggregates could recruit Rnq1 or Sup35 to form ring/ribbon/rod-like (ribbon-like hereafter) heterogeneous aggregates in [*SWI*$^{+}$] cells that are prionogenic, i.e. capable of leading to the formation of [*RNQ*$^{+}$] or [*PSI*$^{+}$] (Du & Li, 2014, Du *et al.*, 2014). In addition, we also reported an antagonizing effect between [*SWI*$^{+}$] and [*PIN*$^{+}$] that [*SWI*$^{+}$] can reduce [*PSI*$^{+}$] promoting capacity of [*PIN*$^{+}$] (Du & Li, 2014). These results demonstrate that the [*SWI*$^{+}$] prion is an excellent system to study prion-prion interactions. However, the lack of a reliable reporter system that can distinguish [*SWI*$^{+}$] from [*swi*$^{-}$] has hindered our understanding of [*SWI*$^{+}$] *de novo* formation and propagation. For instance, what is the spontaneous frequency of [*SWI*$^{+}$] conversion and will [*SWI*$^{+}$] conversion be affected by preexisting prions or overproduction of Swi1 PrD? Swi1 is an essential transcriptional activator for the expression of flocculin (*FLO*) genes (Mao *et al.*, 2008). Flocculins or adhesins are a group of lectin-like

cell wall proteins that confer a variety of multicellular features in several *Candida albicans* and *S. cerevisiae* strains (Barrales *et al.*, 2008, Barrales *et al.*, 2012, Li & Palecek, 2005). We have recently demonstrated that *FLO* gene expression is absent in [*SWI*$^+$] cells so that [*SWI*$^+$] cells cannot exhibit the multicellular features of flocculation, invasive growth or pseudohyphal formation (Du *et al.*, 2015). In this study, by taking advantage of the tight regulation of [*SWI*$^+$] on *FLO* gene expression, we explored the possibility of developing useful [*SWI*$^+$] reporters that can report the prion status of Swi1 and be easily assayed. We report here that we have established several *FLO* promoter-based *URA3* systems (*FLOpr-URA3*) that can be useful for [*SWI*$^+$] research. With these reporters, we have characterized the [*SWI*$^+$] propagation features with a focus on a strain-specific response of [*SWI*$^+$] to functional alterations of Hsp104 and Hsp70-Ssa nucleotide-exchange-factor (NEF) co-chaperone Sse1. These reporter systems have also allowed us to monitor the events of [*SWI*$^+$] *de novo* formation. We have determined and compared [*SWI*$^+$] *de novo* formation frequencies in strains of S228C and 74D-694, and examined the influence of heterologous prions and overproduction of Swi1-PrD on such [*SWI*$^+$] *de novo* formation and the underlying interacting mechanisms driving yeast prion *de novo* formation.

Results

Constructing URA3-based [SWI$^+$] reporters using FLO gene promoters

The yeast S288C strain has two active flocculins, Flo1 and Flo11, which are encoded by two *FLO* genes, *FLO1* and *FLO11,* respectively, and whose functions are essential for exhibiting the multicellular phenotypes of this strain (Kobayashi *et al.*, 1999). Due to containing an internal in-frame stop at codon 142 in the *FLO8 gene*, S288C-derived strains do not express *FLO1* or *FLO11* and thus cannot exhibit certain multicellular phenotypes (Liu *et al.*, 1996). Flo8 is a key transcriptional activator in the cyclic adenosine monophosphate-dependent protein kinase A (cAMP-PKA) pathway and it acts in concert with other activators such as Mga1 and Mss11 in activating *FLO* promoters (Bester *et al.*, 2006, Kim *et al.*, 2014, Mayhew & Mitra, 2014). Upon repair of *FLO8,* the expression of *FLO1* and *FLO11* can be activated and multicellular phenotypes can be restored, such as flocculation and adhesive growth of haploid cells, as well as pseudohyphal growth of diploid cells (Fichtner *et al.*, 2007). Our recent observations that in *FLO8*-repaired S288C strains that Swi1 is required for *FLO* gene expression and [*SWI*$^+$] cells completely lack multicellularity encouraged us to test the idea of developing simple reporter assays of [*SWI*$^+$] using the *FLO* promoters. Since the *FLO1* promoter contains multiple reported interaction sites for SWI/SNF which can be > 5 kb upstream of the *FLO1* start codon (Fleming & Pennings, 2001), it is difficult to clone or engineer the *FLO1* promoter for this purpose. We thus focused on the *FLO11* promoter in this study. As shown in Figure 1A, the *FLO11* promoter contains multiple defined upstream activation sequences (UASs) and upstream repression sequences (URSs), which span a region of about 2.8 kb before the translation start codon (Rupp *et al.*, 1999). Although published data showed that these UASs within the *FLO11* promoter could respond independently to diverse external and internal signals, determination of the SWI/SNF-acting UASs was reported to be difficult (Rupp *et al.*, 1999, Braus *et al.*, 2003, Basu *et al.*, 2004). Since Swi1 is required to activate *FLO11* gene expression (Basu *et al.*, 2004, Du *et al.*, 2015), we assumed that the SWI/SNF (thus, Swi1)-acting sites are within the previously

identified UASs but not URSs. To identify Swi1-acting sites, we generated six truncated *FLO11* upstream regulatory region containing various numbers of UASs (+) and/or URSs (−) by PCR (Figure 1A and S1), and cloned them into the upstream of *URA3* ORF in a *p415*-based plasmid harboring a *CYC1* terminator. In these transcriptional fusion constructs, 50-bp of left and right sequences corresponding to the upstream and downstream regions of the *LYS2* ORF are included to flank the expression cassette, which can be used for integrating the reporter into the *LYS2* locus (Figure 1B).

To test if these reporter plasmids can be used for [*SWI*$^+$] study, we first compared their *URA3* expression in wild-type, single, and double mutant strains of *flo8* and *swi1Δ* (Figure 1C). Except for P_{F16}, a 1.2kb fragment from the 5′- site of the *FLO11* start codon containing 4 UASs and 2 URSs, all tested truncations supported cell growth on media without uracil in the wild-type strain *(FLO8/SWI1)*, suggesting that the two URSs at the region of −600 to −1000bp confer a strong repression. Considering P_{F19} behaved similarly to the wild-type *FLO11* promoter (P_{FLO11}), the 2000-bp upstream sequence of *FLO11* seems to contain most of the critical regulatory elements in S288C strains. The fact that P_{F19} and the wild-type *FLO11* were the only two inactive promoters in *flo8* or *swi1Δ* mutant strain suggests that their de-repression requires both functions of Flo8 and Swi1. The activity of P_{F13} was slightly reduced in *swi1Δ* but not in the *flo8* strain, suggesting that Swi1 but not Flo8 plays a major activator role in interacting with the UASs between −1 and −600bp. It was previously reported that that P_{F13} may serve as a core promoter containing the basal regulatory sites (Braus *et al.*, 2003). Indeed, the activities of P_{F136}, P_{F139}, and P_{F1369}, which contain one or two more activator binding sites beyond P_{F13}, exhibited no significant enhancement of activity comparing to that of P_{F13} in the wild-type strain (Figure 1C). Based on the activities of P_{F16} and P_{F19}, one may speculate that the region of −1600 and −2000 must contain UASs that interact with both Swi1 and Flo8 to de-repress the URSs between −600 and −1000 as P_{F16} grew poorly in SC-ura in all strain backgrounds, however, P_{F19} grew well in the wild-type strain, but not in any of the mutant strains (Figure 1C). Importantly, promoters other than P_{F19} and P_{FLO11} showed significant activities in single mutant strains (Figure 1C), suggesting that Flo8 and Swi1 likely have redundant functions in activating some of the truncated *FLO11* promoters. Taken together, these results demonstrate a complex regulation of *FLO11* promoter by SWI/SNF and Flo8, particularly of the Swi1 responding cis-elements of the promoter.

We next examined if plasmids built with the aforementioned truncated *FLO11* promoters and three additional SWI/SNF-regulated promoters, *SL (a chimeric SUC2-Leu2 promoter)* (Neigeborn & Carlson, 1987), Alcohol DeHydrogenase II (*ADH2)* (Biddick *et al.*, 2008), and HOmothallic switching endonuclease (*HO)* (Stern *et al.*, 1984) (P_{LS}, P_{ADH2}, and P_{HO}), can be used to distinguish [*SWI*$^+$] from [*swi*$^-$] in S288C cells using the uracil/5-FOA growth assay. We also included a growth assay in raffinose media as an additional criterion to monitor the [*SWI*$^+$] status as we previously showed that [*SWI*$^+$] cells grow poorly in media using raffinose as the sole carbon source (Du *et al.*, 2008). Isogenic [*SWI*$^+$], [*swi*$^-$], and *swi1Δ* strains with or without *FLO8* repair were used in these assays. As shown in Figure S2, only two constructs, P_{F19}-*URA3* and P_{F139}-*URA3,* were potentially able to serve as [*SWI*$^+$] reporters. In the presence of Flo8, P_{F19}-*URA3* allowed non-prion ([*swi*$^-$]) cells to grow in −uracil media but not +5-FOA media, whereas [*SWI*$^+$] and *swi1Δ* cells could only

grow in +5-FOA media but not in −uracil media (Figure 1D and S2). Differently, P_{F139}-*URA3* only allowed [*SWI*$^+$]/*swi1Δ* - dependent growth in +5-FOA assay and such a growth phenotype was not *FLO8*-dependent. However, the −uracil growth assay of P_{F139}-*URA3* could not differentiate [*swi*$^-$] cells from cells harboring [*SWI*$^+$] either in the presence or absence of Flo8 (Figure 1D and S2). These results confirmed that both P_{F19}-*URA3* and P_{F139}-*URA3* could be potentially useful for [*SWI*$^+$] study under selective conditions. We next investigated if we could establish a stable, chromosomal reporter of P_{F139}-*URA3* by replacing the endogenous *FLO11* gene (including both the promoter region and ORF, see Experimental Procedures for details) at the *FLO11* locus. Unexpectedly, the chromosomal P_{F139}-*URA3* (*Chr::*P_{F139}-*URA3*) behaved differently from its plasmid version (compare Figure 1D and S3) – it could only discriminate [*SWI*$^+$] and [*swi*$^-$] in the −uracil assay in the presence of *FLO8* but not in the +5-FOA assay in either *flo8* or *FLO8* background (Figure S3). As we showed previously (Du *et al.*, 2015), *Chr::*P_{FLO1}-*URA3* can clearly distinguish [*SWI*$^+$] and [*swi*$^-$] cells in both −uracil and +5-FOA assays (Figure S3) and thus it is, applicable as a useful [*SWI*$^+$] reporter. The *Chr::*P_{FLO11}-*URA3* behaves similarly to its plasmid version, which could only be used in the −uracil assay. After all, in above uracil/5 FOA assays, *swi1Δ* and [*SWI*$^+$] strains could be noticeably distinguished by using some but not all of the reporter constructs, the [*SWI*$^+$] status should be further verified by other reversible features such as aggregation and raffinose utilization.

Suitability of P_{F139}- and P_{F19}-URA3 reporters in [SWI$^+$] research for the 74D-694 strain derivatives

Next, we investigated if P_{F19}-*URA3* and P_{F139}-*URA3* could be used as [*SWI*$^+$] reporters in 74D-694 strain and derivatives, which are commonly used for yeast prion studies. Upon examination, we found that the 74D-694 strain does not display multicellular phenotypes (data not shown), suggesting that the *FLO* genes are not expressed. DNA sequencing data demonstrated that the *FLO8* gene contains a point mutation in the code of the 142th amino acid (tryptophan) to a stop code, which is identical to that in S288C strain (Figure 2A). Thus, the lack of multicellularity of 74D-694 is due to the same *flo8* mutation of S288C. We transformed a plasmid expressing *FLO8* into a wild-type 74D-694 strain and tested if *FLO8* expression could restore the multicellular features, and if so, would these phenotypes be regulated by [*SWI*$^+$]. We found that ectopic expression of *FLO8* driven by its own promoter from a *CEN*-plasmid successfully restored the multicellular phenotypes of adhesive growth (Figure 2B) and flocculation (Figure 2C). Both phenotypes were abolished by [*SWI*$^+$] but not by [*PSI*$^+$] or [*PIN*$^+$]. Taken together, we concluded that similar to S288C, the 74D-694 strain contains a mutation in *FLO8* and thus lacks multicellularity; repairing Flo8 restores *FLO* gene expression and multicellularity; and [*SWI*$^+$] abolishes *FLO* gene expression and multicellularity.

To test if P_{F19}-*URA3* and P_{F139}-*URA3* could be used to report the [*SWI*$^+$] state in 74D-694 strains, we tested four isogenic 74D-694 strains harboring different prions (Figure 2D). As shown in Figure 2E, P_{F139}-*URA3* allowed [*SWI*$^+$] cells to grow on 5-FOA-containing media but not on −uracil media, whereas [*PSI*$^+$], [*PIN*$^+$], and non-prion ([*psi*$^-$][*pin*$^-$][*swi*$^-$]) strains grew well in −uracil media but had no growth in +5-FOA media. Interestingly, these phenotypes are independent of *FLO8* (Figure 2E), indicating that P_{F139}-*URA3* can serve as a

[*SWI*$^+$]-specific reporter for 74D-694 strains in the presence or absence of *FLO8*. For P_{F19}-*URA3,* all tested strains did not grow on media lacking uracil without ectopic *FLO8* expression, whereas *FLO8* expression allowed growth on −uracil media for [*PSI*$^+$], [*PIN*$^+$], and [*swi*$^-$] but not for [*SWI*$^+$] cells that were the only ones growing on +5-FOA plates (Figure 2F). These results demonstrate that P_{F19}-*URA3* can be a faithful [*SWI*$^+$] reporter for 74D-694 strains in the presence of functional Flo8.

Although the P_{F139}-*URA3* reporter can be a decent [*SWI*$^+$] reporter only in +5-FOA assay for S288C strains without Flo8 ectopic expression, it can be used in both −uracil and 5-FOA assays for 74D-694 strains independent of Flo8 expression (compare Figure 1D and 2E). However, P_{F19}-*URA3* can be used in either −uracil or +5-FOA assay for both S288C and 74D-694 strains only when Flo8 is ectopically expressed. These results demonstrate strain-specific performance of the two reporters.

Influence of Sse1-overproduction and its interaction with Hsp104 on [SWI$^+$] propagation

The maintenance of a yeast prion requires a concerted action from multiple molecular chaperones and other cellular factors (Winkler *et al.*, 2012, Masison & Reidy, 2015). It was reported earlier that Sse1 overproduction can eliminate [*SWI*$^+$] in 74D-694 strain whereas Hsp104 overproduction cannot (Du *et al.*, 2008, Hines *et al.*, 2011). To validate the suitability of the plasmid-based P_{F139}-*URA3* reporter in [*SWI*$^+$] study, we examined if this reporter plasmid could be used to study the curing of [*SWI*$^+$] by 5-mM guanidine hydrochloride (GdnHCl), a treatment known to eliminate [*SWI*$^+$] through inactivating Hsp104 (Du *et al.*, 2008). When [*SWI*$^+$] S288C strains containing the P_{F139}-*URA3* plasmid were treated with 5-mM GdnHCl, the reporter plasmid was effective in detecting the [*SWI*$^+$] curing as demonstrated by a lack of growth in +5-FOA media for both *flo8* and *FLO8* strains (Figure 3A). The 1.0 mg/mL 5-FOA concentration showed clear delineation between the prion and cured conditions and was used in the rest of the experiments described in this article.

Experiments were conducted using the P_{F139}-*URA3* reporter plasmid in both 74D-694 and BY4741 (S288C derivative) strains. As expected, [*SWI*$^+$] was eliminated by GdnHCl treatment but not by Hsp104 overproduction in both strains; however, unexpectedly, Sse1 overproduction only cured [*SWI*$^+$] in 74D-694 but not the same [*SWI*$^+$] variant in BY4741 (Figure 3B and 3C). To verify these results, experiments were repeated with a *FLO8*-repaired S288C [*SWI*$^+$] strain with an integrated copy of P_{FLO1}-*URA3* at the *FLO1* locus (Du *et al.*, 2015). As shown in Figure 3D, similar results were obtained. These results indicate that [*SWI*$^+$] is sensitive to Sse1 overproduction only in 74D-694 but not in S288C.

The insensitivity of [*SWI*$^+$] to Sse1 overproduction in S288C background suggests a possibility that Sse1 does not participate in [*SWI*$^+$] propagation in S288C since additional nucleotide exchange factors for Hsp70 do exist, such as Sse2 and Fes1 (Kabani *et al.*, 2002, Mukai *et al.*, 1993). To test this likelihood, we examined if Hsp104 or Sse1 overproduction would affect the [*SWI*$^+$] curing capacity of GdnHCl using the chromosomal P_{FLO1}-*URA3* reporter in a S288C [*SWI*$^+$] strain. Hsp104 and Sse1 were individually overproduced under a GPD promoter in media containing 5 mM GdnHCl. After expression and curing, [*SWI*$^+$] loss was estimated by phenotypic assays on −uracil, +5-FOA, and raffinose plates. As shown

in Figure 3E, overproduction of Hsp104 or Sse1 significantly delayed the prion curing process by GdnHCl. For instance, after 24 h of growth, there are larger fractions of cells overexpressing *SSE1* or *HSP104* retaining [*SWI*$^+$] compared to that of the vector control (Figure 3E). As expected, excess amount of Hsp104 can antagonize the inactivating effect of GdnHCl. It is noteworthy that Sse1 showed a greater antagonizing effect against the prion curing by GdnHCl than Hsp104 overproduction. Although it is unclear why Sse1 overproduction decreases [*SWI*$^+$]-curing capacity of GdnHCl, our results suggest that Sse1 does participate in [*SWI*$^+$] maintenance and propagation via direct or indirect interaction with Hsp104, and a higher expression level of Sse1 favors [*SWI*$^+$] propagation in the S288C strain derivatives (compare Figure 3B-3E).

The effects of strain, heterologous prions, and Swi1 PrD overproduction on [SWI$^+$] formation

As the [*SWI*$^+$] formation frequency remained elusive, next, we investigated the spontaneous rate of [*SWI*$^+$] conversion in S288C and 74D-694 strains. For S288C, the *FLO8*-repaired BY4741*FLO8::HIS3 flo1::P$_{FLO1}$-URA3* non-prion ([*psi*$^-$][*pin*$^-$][*swi*$^-$]) strain was used because the integrated *P$_{FLO1}$-URA3* reporter is a better [*SWI*$^+$] reporter compared to *P$_{F139}$-URA3* for this strain background (Figure S3 and 1D). The 5-FOA resistant (5-FOA$^+$) colonies were screened and then examined for their curability by 5 mM GdnHCl (Figure 4A and data not shown). Candidates that were able to convert from Ura$^-$ 5-FOA$^+$ Raf$^\pm$ to Ura$^+$ 5-FOA$^-$ Raf$^+$ upon a treatment via growth on 5 mM GdnHCl plates were assayed for aggregation after being transformed with *p415TEF-NQYFP,* a plasmid expressing a -YFP fusion of N-terminal region of Swi1 containing the first 524 amino acid residues of Swi1 that is asparagine (N) and glutamine (Q)-rich. Only those 5-FOA$^+$ isolates that displayed NQ-YFP aggregation and were GdnHCl-curable were scored as [*SWI*$^+$]. As shown in Figure 4B, the average spontaneous [*SWI*$^+$] formation frequency was approximately 5×10^{-4} for S288C under the examined experimental conditions.

For 74D-694, we showed that the *P$_{F139}$-URA3* reporter allows 74D-694 [*SWI*$^+$] cells to grow in 5-FOA independent of Flo8 (Figure 2E). To monitor [*SWI*$^+$] spontaneous formation rate in 74D-694, isogenic [*PSI*$^+$], [*PIN*$^+$], and non-prion ([*psi*$^-$][*pin*$^-$][*swi*$^-$]) strains of 74D-694 were co-transformed with *p415F139-URA3* and *p413GAL1-NQYFP,* and screened for growth on +5-FOA plates. Using the aforementioned criteria, 5-FOA$^+$ colonies that exhibited NQ-YFP aggregation upon galactose induction and were curable by GdnHCl were scored as [*SWI*$^+$] (Figure 4C). Regarding this, addition of 0.01 - 0.1% of galactose in sucrose-based media was sufficient to give rise to an aggregation frequency of about 30-80% for N-YFP (a YFP fusion containing the first 323 amino acids of Swi1 that are asparagine-rich and responsible for [*SWI*$^+$] prion phenotypes) and NQ-YFP when expressed from a *CEN*-plasmid in [*SWI*$^+$] cells, and no aggregation was detectable in [*swi*$^-$] cells (Figure S4 and data not shown). Thus, 0.02% galactose serves as minimal concentrations to show [*SWI*$^+$]-specific Swi1 N or NQ-YFP aggregation (Figure S4). Isolates with NQ-YFP aggregation were further colony-purified and re-assayed for aggregation stability, growth phenotypes on −uracil, +5-FOA, and raffinose plates, and curability by 5 mM GdnHCl (Figure 4C and data not shown).

As shown in Figure 4B, the spontaneous [*SWI*$^+$] conversion frequency of 74D-694 is about 4×10^{-5} – approximately 10x lower than that of S288C under identical experimental conditions. Moreover, the tested [*PSI*$^+$] and [*PIN*$^+$] 74D-694 strains gave [*SWI*$^+$] spontaneous formation frequency of about 4×10^{-3} and 4×10^{-4}. Even though such an estimation of [*SWI*$^+$] frequencies in [*PSI*$^+$] and [*PIN*$^+$] cells can be rough considering the possibility that the combination of [*SWI*$^+$] with [*PSI*$^+$] or [*PIN*$^+$] may affect the fitness of cells carrying certain [*SWI*$^+$] variants, our results suggest the [*SWI*$^+$] conversion frequencies are approximately 100x and 10x greater in the [*PSI*$^+$] and [*PIN*$^+$] strains than that of the non-prion strain, respectively (Figure 4B). These data indicate that [*PSI*$^+$] and [*PIN*$^+$] can significantly promote [*SWI*$^+$] *de novo* conversion. The unexpected observation that [*PSI*$^+$] has a significantly higher inducibility of [*SWI*$^+$] than [*PIN*$^+$] suggests that the two prions might be structurally different and thus have different capability of cross-seeding Swi1 toward [*SWI*$^+$] formation. Since [*SWI*$^+$] could also promote [*PSI*$^+$] and [*PIN*$^+$] *de novo* formation (Du & Li, 2014), [*SWI*$^+$], [*PSI*$^+$], and [*PIN*$^+$] seem to facilitate each another's conversions. Ribbon-like NQ-YFP aggregation patterns were frequently observed in the newly formed [*SWI*$^+$] cells and gradually lost and turned to dots upon a colony-purification process (Figure 4C). This is quite similar to the aggregation pattern changes of Sup35 and Rnq1 in the prionogenesis of [*PSI*$^+$] and [*PIN*$^+$] (Du & Li, 2014, Mathur *et al.*, 2010, Zhou *et al.*, 2001).

Next, we asked if overproduction of the Swi1 PrD would promote [*SWI*$^+$] *de novo* formation. We showed previously that the first 323-amino acid of Swi1 (Swi1-N) contains the Swi1 PrD [57]. When Swi1-N was over-expressed under the *TEF1* promoter from a *CEN*-plasmid in 74D-694 strains carrying the P_{F139}-*URA* plasmid, we obtained significantly more 5-FOA$^+$ colonies when compared to that of the vector control (data not shown). To better investigate the interplay between Swi1-N overproduction and heterologous prion interactions in regard to [*SWI*$^+$] formation, we utilized N-YFP expression under the *GAL1* promoter with supplementation of 0.5% galactose. The obtained 5-FOA$^+$ colonies that exhibited GdnHCl-curable N-YFP-aggregation and growth phenotypes of Raf$^\pm$, Ura$^-$, and 5-FOA$^+$ were scored as [*SWI*$^+$]. As shown in Figure 5A, without N-YFP overproduction, the [*SWI*$^+$] *de novo* forming frequencies were comparable to that shown in Figure 4B, however, the [*SWI*$^+$] conversion rates were significantly increased by N-YFP overproduction. Interestingly, although [*PSI*$^+$] has a considerably higher promoting ability for spontaneous [*SWI*$^+$] formation than [*PIN*$^+$], its capability of promoting [*SWI*$^+$] formation under the N-YFP overproduction condition is similar to that of [*PIN*$^+$] (comparing Figure 4B to 5A). In this case, N-YFP overproduction gave rise to [*SWI*$^+$] forming frequencies of about 6.7x, 39.3x and 27.5x higher than the spontaneous frequencies for [*PSI*$^+$], [*PIN*$^+$], and non-prion strains, respectively (Figure 5A).

Interacting mechanisms in spontaneous and pre-existing prion-induced [SWI$^+$] initiation

Protein misfolding and aggregation are critical events that lead to prionogenesis (Landreh *et al.*, 2016). Upon overproduction prionogenic aggregations of Sup35 and Rnq1 often occur and appear to be ring/ribbon-shaped (Zhou *et al.*, 2001, Mathur *et al.*, 2010, Du *et al.*, 2014). Ring/ribbon-like aggregation was also seen for other prion and prion-like proteins [18]. As shown in Figure 4C, similar to the *de novo* formation of [*PSI*$^+$] and [*PIN*$^+$], Swi1 also

appears primarily as ring/ribbon-like aggregates in premature [*SWI*$^+$] cells and became dot-like in mature [*SWI*$^+$] cells. To understand how [*PSI*$^+$], [*PIN*$^+$], and Swi1 PrD overproduction promotes [*SWI*$^+$] *de novo* formation, we further investigated aggregation and interactions of Swi1 with Sup35 and Rnq1 in the process of [*SWI*$^+$] initiation and maturation. To do so, Swi1-N-mCherry and Sup35 NM-GFP were co-expressed from the *GAL1* and *CUP1* promoters, respectively, in a [*PSI*$^+$] or non-prion 74D-694 strain; *GAL1*-Swi1-N-mCherry and *CUP1*-Rnq1-GFP were similarly co-expressed in a [*PIN*$^+$] or non-prion 74D-694 strain. Galactose was added to a final concentration of 0.02% as a minimal amount to visualize N-mCherry aggregation in [*SWI*$^+$] cells, and this very low galactose induction condition will be referred to as non-overproduction (or low N-mCh) hereafter. In parallel, conditions using 0.5% galactose are referred to as overproduction (or high N-mCh). Similarly, we observed that 10 μM $CuSO_4$ is the lowest concentration necessary to see Sup35 NM-GFP aggregation in [*PSI*$^+$] cells (Figure S5). Therefore, such a minimal $CuSO_4$ concentration was used to visualize Sup35 NM-GFP and Rnq1-GFP aggregation in [*PSI*$^+$] and [*PIN*$^+$] cells without unnecessary overproduction.

In the non-overproduction condition (0.02% galactose), the presence of [*PSI*$^+$] or [*PIN*$^+$] significantly increased both total and ring/ribbon-like aggregation of N-mCherry (Figure 5B). When compared to the non-prion cells, [*PSI*$^+$] and [*PIN*$^+$] cells had 5.2x and 10.7x more total aggregation of N-mCherry, respectively (Figure 5B). These results are consistent with the result of a higher [*SWI*$^+$] conversion rate in [*PSI*$^+$] or [*PIN*$^+$] cells than that of non-prion cells (Figure 4B and 5A). The ring/ribbon-like aggregates of N-Cherry accounted for ~88%, 77%, 97%, and 86% of the total N-mCherry aggregates in [*PSI*$^+$] cells expressing Sup35 NMGFP, non-prion expressing Sup35 NMGFP, [*PIN*$^+$] cells expressing Rnq1GFP, and non-prion cells expressing Rnq1GFP, respectively. These results show that Swi1 aggregates are predominantly ring/ribbon-like at the [*SWI*$^+$] initiation stage. Remarkably, only a small fraction of the N-mCherry aggregates are heritable to become mature [*SWI*$^+$] whereas > 90% of them were ultimately lost (calculated by dividing the percent frequency of [*SWI*$^+$] isolates (Figure 5A) by the percent frequency of total aggregates (Figure 5B and 5C). This result suggests that even though the ring/ribbon-like Swi1 aggregation was attributable to [*SWI*$^+$] formation, most of the initially formed ribbon-like Swi1 aggregates could not lead to [*SWI*$^+$] formation but are rather off-pathway products. Interestingly, although [*PSI*$^+$] cells had a nearly 10x higher spontaneous [*SWI*$^+$] formation rate than that of [*PIN*$^+$] cells, [*PSI*$^+$] cells overall had lower ring/ribbon-like aggregation of N-mCherry (compare Figure 5A and 5B). These results suggest that the [*PSI*$^+$]-induced Swi1 aggregation is more prionogenic than that induced by [*PIN*$^+$].

As expected, Swi1 PrD overproduction (0.5% galactose) promoted the total and ring/ribbon-like aggregation of N-mCherry (compare Figure 5B and 5C). Importantly, Swi1 PrD overproduction-induced N-mCherry aggregation is predominantly ring/ribbon-like (Figure 5C), which was consistent with the capacity of Swi1 PrD in promoting [*SWI*$^+$] formation (Figure 5A). Although the dominance of ring/ribbon-like aggregation is relatively low under overproduction conditions compared to that under non-overproduction (compare Figure 5B and 5C), there were about 28.7%, 11.9%, and 0.17-8.5% of [*PSI*$^+$], [*PIN*$^+$], and non-prion cells, respectively, containing N-mCherry ring/ribbon-like aggregates that eventually became [*SWI*$^+$] isolates under Swi1 PrD overproduction, which is much greater than their non-

overproduction controls ([*PSI*$^+$], 5.9%; [*PIN*$^+$], 0.75%; non-prion, 0.4-0.67%). The aforementioned values were calculated by dividing the percent frequency of [*SWI*$^+$] isolates (Figure 5A) by the percent frequency of ribbon-like aggregates (Figure 5B and 5C). Noticeably, [*PSI*$^+$] cells generated approximately 21x more [*SWI*$^+$] than the non-prion control with Swi1 PrD overproduction though the two strains showed similar amount of ring/ribbon-like aggregation of N-mCherry (Figure 5A and 5C). This again suggests that the Swi1 ring/ribbon-like aggregates formed in [*PSI*$^+$] cells were more prionogenic. In other words, the Swi1 ring/ribbon-like aggregates formed in the [*PIN*$^+$] and nonprion strains were less prionogenic or a larger fraction of such aggregates were off-pathway products compared to those formed in the [*PSI*$^+$] strain. Taken together, these data suggest that the promotion of [*SWI*$^+$] conversion by a preexisting prion, such as [*PSI*$^+$] or [*PIN*$^+$], or an event of Swi1-PrD overproduction, is achieved by facilitating Swi1 aggregation, including the ring/ribbon-like aggregation.

In the same experiments, we further assayed the interaction of Swi1 N-mCherry ring/ribbon-like aggregates with Sup35 NM-GFP and Rnq1-GFP under non-overproduction conditions and observed both colocalization (cross-seeding) and non-colocalization patterns for all tested strains (Figure 6A, 6B and data not shown). For instance, after 48 h of induction, about 94% and 90% of N-mCherry ribbon-like aggregates co-localized with Sup35 NM-GFP and Rnq1-GFP in [*PSI*$^+$] and [*PIN*$^+$] cells, respectively, in which the two preexisting prion aggregates were morphologically remodeled from dot-shaped to ring/ribbon/rod-like. Similarly, about 63% and 59% of Swi1 N-mCherry ring/ribbon-like aggregates co-localize with the signals of Sup35 NM-GFP and Rnq1-GFP in non-prion cells, respectively (Figure 6AC and 6B). Though colocalization signals of N-mCherry to Sup35 NM-GFP and Rnq1-GFP were prevalent in non-prion cells, the extremely low spontaneous aggregation frequency (Figure 5B) explains the low rate of [*SWI*$^+$] conversion in this strain. These data suggest that under a Swi1 PrD non-overproduction condition, cross-seeding by Sup35 or Rnq1 is a major mechanism in promoting Swi1 aggregation and [*SWI*$^+$] formation in all strains examined. However, a pre-existing [*PSI*$^+$] or [*PIN*$^+$] might provide a larger amount of ready-to-go templates for efficient cross-seeding of Swi1 to produce more on-pathway products to promote [*SWI*$^+$] formation.

Under the overproduction condition of Swi1 PrD, there were approximately 88% and 93% N-mCherry ring/ribbon-like aggregates co-localized with the morphologically remodeled Sup35 NM-GFP and Rnq1-GFP in [*PSI*$^+$] and [*PIN*$^+$] cells, respectively (Figure 6A and 6B), whereas there were only about 8% and 16% of the total N-mCherry ring/ribbon-like aggregates co-localized with Sup35 NM-GFP and Rnq1-GFP in non-prion cells, respectively (Figure 6A and 6B). These results suggest that in the event of Swi1 PrD-overproduction-promoted [*SWI*$^+$] formation, cross-seeding is a major interacting mechanism between Swi1 and Sup35 or Rnq1 in [*PSI*$^+$] and [*PIN*$^+$] cells, but not in the examined non-prion cells under identical experimental conditions.

Sup35 and Rnq1 share similar mechanistic features in interacting with Swi1 in their prionogenesis processes

We showed previously that [*SWI*$^+$] can promote [*PSI*$^+$] and [*PIN*$^+$] *de novo* formation (Du & Li, 2014). To examine the prionogenesis process of [*PSI*$^+$] and [*PIN*$^+$] by a preexisting [*SWI*$^+$], we transformed a [*SWI*$^+$] 74D-694 strain with *p423GAL1-N-mCherry* and *pCUP1NMGFP* or *pCUP1RNQ1GFP*. Upon addition of 10 μM $CuSO_4$ and 0.02% galactose, an induction condition sufficient for visualizing prion protein aggregation without a significant overproduction, we examined the interactions of Swi1-N-mCherry with Sup35 NM-GFP and Rnq1-GFP. As shown in Figure 6C, under this induction condition, > 90% of Sup35 NM-GFP and Rnq1-GFP aggregates had ring/ribbon-like pattern and were co-localized with Swi1 N-mCherry aggregates, which were apparently remodeled from dot-shaped to ring/ribbon-like. These data indicate that cross-seeding is also a dominant interacting mechanism for [*SWI*$^+$] to facilitate the conversion of [*PSI*$^+$] and [*PIN*$^+$] under non-overproduction conditions. With overproduction of Swi1 PrD (0.5% galactose) in pre-existing [*SWI*$^+$] cells, the initially formed Sup35 NM-GFP and Rnq1-GFP ring/ribbon-like aggregates were also mostly colocalizing with morphologically remodeled Swi1 aggregates as we previously reported (Du & Li, 2014). In non-prion cells, when Swi1 N-mCherry was overproduced in the presence of 0.5% galactose, we found that Sup35 NMGFP and Rnq1-GFP ribbon-like aggregates rarely co-localize with Swi1 N-mCherry. In this case, only about 15% and 23% of the total ribbon-like aggregates of Sup35 NM-GFP and Rnq1-GFP colocalized with Swi1 N-mCherry, respectively (Figure 6C), suggesting that cross-seeding of Swi1 with Sup35 and/or Rnq1 rarely occurs in prionogenesis promoted merely by overproduction without a preexisting prion. Taken together, Sup35 and Rnq1 share similar interacting mechanistic features with Swi1 at their prion initiation stage.

Discussion

Based on our previous report that [*SWI*$^+$] tightly regulates the expression of *FLO* genes that are essential for yeast multicellularity (Du *et al.*, 2015), we have dissected the *FLO11* promoter through a serial truncation analysis with the goals of understanding the *FLO11* regulation by SWI/SNF and establishing a simple, faithful reporter system for [*SWI*$^+$] study. As shown in Figure 1-2, we identified several truncated variants of the *FLO11* promoter that can report the prion status of Swi1. Interestingly, we also uncovered a strain-specific requirement of Flo8 on some of the truncated *FLO11* promoter variants. For example, P_{F19}-*URA3* can select for [*swi*$^-$] cells using SC-ura media for both strains of 74D-694 and S288C but only in the presence of *FLO8,* whereas P_{F139}-*URA3* can select for [*SWI*$^+$] cells using media supplemented with 5-FOA in the presence or absence of *FLO8* for the 74D-694 strain. To be able to select for [*SWI*$^+$] cells in the absence of a functional Flo8 in 74D-694 enabled us to estimate the spontaneous rate of [*SWI*$^+$] formation by simply analyzing *de novo* formed 5-FOA$^+$ isolates in any 74D-694 strain-derivatives without *FLO8* repair. We show here that the spontaneous formation rate of [*SWI*$^+$] is about 10^{-5} to 10^{-4} (Figure 4B), which is significantly higher than that of [*PSI*$^+$], ~ 5×10^{-7} (Lancaster *et al.*, 2010), but comparable to the observed rates for [*ISP*$^+$] (Rogoza *et al.*, 2010, Volkov *et al.*, 2002), [*MOT3*$^+$] (Alberti *et al.*, 2009), and [*URE3*] (Brachmann *et al.*, 2006, Wickner, 1994, Aigle & Lacroute, 1975), which can also be as high as 10^{-4}. Previously, the rate of spontaneous

formation of [*RNQ*$^+$] ([*PIN*$^+$]) was reported as ~ 2.96×10^{-6} (Huang *et al.*, 2013). Interestingly, the protein determinants of [*SWI*$^+$], [*URE3*], [*MOT3*$^+$], and [*ISP*$^+$] prions are low abundant transcriptional regulators with an asparagine (N)-rich PrD whereas the protein determinants of [*PSI*$^+$] and [*PIN*$^+$] prions are abundant cytoplasmic proteins with a PrD rich in both glutamine and asparagine (Q/N). It seems our newly determined spontaneous formation rate of [*SWI*$^+$] is in agreement with an earlier prediction that PrDs with higher Q/N ratios seem to give rise to higher numbers of seeds (i.e. aggregates that can act as a template for the prion form) but lower prion formation rates whereas PrDs with lower Q/N ratios may give lower seed numbers but higher prion formation rates (Hines & Craig, 2011, Hines *et al.*, 2011). However, the rate of a prion may be variable under different conditions, such as, in the absence of [*PIN*$^+$], the [URE3] rate can be 10 fold lower (Bradley *et al.*, 2002). Further research is needed to verify above observations and test the accuracy of the prediction.

Molecular chaperones are usually proteins that assist folding of nascent proteins and/or unfolding of mis-folded proteins. It has been shown that different prions can interact differently with molecular chaperones which are necessary for prion formation and propagation. For example, Hsp104 is needed for fragmentation of larger amyloid fibrils to produce prion seeds essential for prion propagation. Actually, Hsp104 overproduction can eliminate [*PSI*$^+$] but has no effect on other prions (Crow & Li, 2011, Chernoff *et al.*, 1995), and some N-rich prions, such as [*URE3*] and [*SWI*$^+$], are sensitive to functional alterations of Hsp70-Ssa and its co-chaperones. The N-rich prions can be cured by Hsp70-Ssa overproduction, Sse1 overproduction, *SSE1* deletion, or overproduction of Ydj1 or J-domain containing Hsp40 chaperones, whereas the Q/N-rich prions of [*PSI*$^+$] and [*PIN*$^+$] are generally resistant to such manipulations except weak [*PSI*$^+$] variants that can be cured by *SSE1* deletion (Fan *et al.*, 2007, Hines *et al.*, 2011, Kryndushkin & Wickner, 2007). In addition, [*SWI*$^+$] is uniquely sensitive to Sis1 overproduction and *YDJ1* deletion (Hines *et al.*, 2011). Intriguingly, variants of the same prion can also interact with molecular chaperones dramatically different. For instance, Sse1 is required for propagating a weak [*PSI*$^+$] variant but not for the propagation of a stronger variant under identical experimental conditions (Kryndushkin & Wickner, 2007, Fan *et al.*, 2007). In this study, we also demonstrate a dramatic strain-specific interaction between [*SWI*$^+$] and Sse1, the NEF of Hsp70-Ssa. We show that [*SWI*$^+$] was eliminated by Sse1 overproduction in a 74D-694 strain but the same [*SWI*$^+$] variant in a S288C strain was not (Figure 3B and 3C). Although it is possible that a different NEF other than Sse1, such as Sse2 or Fes1 (Kabani *et al.*, 2002, Mukai *et al.*, 1993), is required for interacting with Hsp70-Ssa for [*SWI*$^+$] maintenance in the S288C strain, our observation that Sse1 is actively engaged in [*SWI*$^+$] seed production in both strains of 74D-694 and S288C (Figure 3B-3E) indicates that it is not the case. The mechanism that underlies this strain-specific interaction of [*SWI*$^+$] and Sse1 remains to be investigated.

Besides PrP^{Sc}, amyloid architecture is shared by a large number of other pathogenic proteins, including α-synuclein, β-amyloid, tau, and TDP-43, each of which is tightly linked to a fatal, devastating neurodegenerative disease (Aguzzi & O'Connor, 2010, Soto, 2003, Eisenberg & Jucker, 2012). As yeast prions are naturally occurring heritable amyloids, the budding yeast becomes a powerful model organism to study the behavior of amyloids.

Although it is known that amyloidogenesis generally initiates from aberrant protein folding and aggregation, molecular events leading to amyloidosis remain poorly understood. In this study, we observed that in both cases of spontaneous [*SWI*$^+$] formation in the absence of a known prion and Swi1-overproduction-facilitated [*SWI*$^+$] conversion, Swi1 aggregates are predominantly ring/ribbon-like at the initiation stage of [*SWI*$^+$] formation, which are then processed to become dot-like in mature [*SWI*$^+$] cells (Figure 4C, 5B and 5C). Similar ribbon-to-dot transition events also take place in the prionogenesis of [*PSI*$^+$], [*PIN*$^+$], and a group of potential Q/N-rich prion candidates when overproduced (Alberti *et al.*, 2009, Zhou *et al.*, 2001, Du & Li, 2014). In the case of [*PSI*$^+$] *de novo* formation, although both ring/ribbon-like and dot-like aggregation may appear upon Sup35 overproduction, only the former is usually prionogenic (Alberti *et al.*, 2009, Derkatch *et al.*, 2001, Zhou *et al.*, 2001). In this study, we also observed that higher [*SWI*$^+$] formation rates are associated with higher rates of ring/ribbon-like Swi1 aggregation (Figure 4B, 5B and 5C). The fact that both ring/ribbon-like and dot-like aggregates of [*PSI*$^+$] share the same bundled fibrillar amyloid structure (Kawai-Noma *et al.*, 2010, Tyedmers *et al.*, 2010) suggests that this morphologic change of aggregation from ribbon-like to dot-like is unlikely to involve any significant changes in prion amyloid structures rather being a result of changes in their association partners.

We show here that the presence of a preexisting prion, [*PSI*$^+$] or [*PIN*$^+$], can facilitate the *de novo* formation of [*SWI*$^+$]. Under Swi1-PrD overproduction conditions, although [*PSI*$^+$] and non-prion strains had similar Swi1 N-mCherry aggregation frequency, the [*PSI*$^+$] strain gave rise to a [*SWI*$^+$] formation rate 21.5x higher than that of the non-prion strain (Figure 5A and 5C). In addition, in a [*PIN*$^+$] strain, Swi1 PrD overproduction-induced N-mCherry aggregation (including total and ring/ribbon-like) and the [*SWI*$^+$] conversion were significantly greater than in an isogenic non-prion strain (Figure 5A and 5C) – confirming that a preexisting prion can promote [*SWI*$^+$] *de novo* formation. Interestingly, without overproduction, the N-mCherry ring/ribbon-like aggregation frequency is lower in [*PSI*$^+$] cells than that in [*PIN*$^+$] cells; however, the [*SWI*$^+$] formation rate is opposite - higher in [*PSI*$^+$] cells but lower in [*PIN*$^+$] cells (Figure 4B and 5B). These data suggest that [*PSI*$^+$] is a better inducer of [*SWI*$^+$] than [*PIN*$^+$]. Although the underlying mechanism of such preferable induction of [*SWI*$^+$] by [*PSI*$^+$] remains to be elucidated, we can speculate that perhaps the [*PSI*$^+$] and [*SWI*$^+$] prions are more structurally compatible than the [*PIN*$^+$] and [*SWI*$^+$] prions are and thus [*PSI*$^+$] is a better cross-seeding template for [*SWI*$^+$]. We also demonstrate here that a larger fraction of Swi1 aggregates are ring/ribbon-like in the non-overproduction condition than observed in N-mCherry overproduction conditions (compare Figure 5B and 5C), indicating that Swi1 PrD overproduction resulted in producing more non-prionogenic, off-pathway aggregation products.

Previous studies suggest that interactions of heterologous prion proteins mainly happen during the early phase of the prionogenesis process of [*PSI*$^+$] and [*PIN*$^+$] (Bagriantsev & Liebman, 2004, Derkatch *et al.*, 2004, Du & Li, 2014). This is further confirmed by our finding that co-localization of Swi1 with Rnq1 or Sup35 mainly takes place at the initial prionogenic stage of [*SWI*$^+$] formation (Figure 4C, 6A and 6B). We also show that with or without overproduction, the initially formed ring/ribbon-like aggregates of Swi1, Sup35, and Rnq1 predominantly overlap with the pre-existing prion facilitator even though some non-

colocalizing aggregation can also occur simultaneously. In a non-prion strain, such a cross-seeding mechanism can also be prevalent without an overproduction event, but it rarely occurs when a prion protein is overproduced. The co-localization predominance of Swi1 with Sup35 or Rnq1 in a [*PSI*$^+$] or [*PIN*$^+$] strain is in agreement with an increase in [*SWI*$^+$] conversion by the preexisting prion. These results suggest that the cross-seeding mechanism of using a pre-existing prion(s) as a template is an efficient means to facilitate the formation of another prion. The mechanistic events of yeast prion formation and interaction described here may have implications on etiologies of mammalian amyloidosis, which is also caused by protein misfolding and aggregation, similar to that of yeast prions (Chiti & Dobson, 2006, Prusiner, 2012, Soto, 2012). Many of these pathogenic proteins contain a Q/N-rich prion-like region (King *et al.*, 2012). Notably, some of these pathogenic proteins often can co-aggregate (Gotz *et al.*, 2001, Guo *et al.*, 2013, Ono *et al.*, 2012). It remains of great interest to understand how cross-seeding and other interaction mechanisms function in the aggregation and co-aggregation events of these pathogenic proteins. Thus the study of yeast prions can provide insights into our understanding of the general mechanisms involved in protein misfolding, aggregation, and protein misfolding diseases.

Experimental Procedures

Oligonucleotides, plasmids, and yeast strains that were used in this study are shown in Table S1, S2, and S3, respectively

Plasmid construction

Plasmids of p413TEF-NYFP, p413TEF-NQYFP, p413GAL1-NYFP, p413GAL1-NQYFP, p423GAL1-NYFP, p423GAL1-NQYFP, p423GPD-NYFP, p425GPD-NQYFP, p425GPD-NYFP, and *p425GPD-SWI1YFP* were constructed by sub-cloning the corresponding *N-YFP*, *NQ-YFP*, and *SWI1-YFP* fragment from *p416TEF-NYFP*, *p416TEF-NQYFP*, and *p416TEF-SWI1-YFP* into empty vectors of *p413TEF*, *p413GAL1*, *p423GAL1*, *p423GPD* and *p425GPD* through sites of *Spe*I/*Xho*I, respectively. A 714-bp *mCherry* PCR product was amplified with primer pair of mCherry-F/mCherry-R using *p413TEF-SWI1mCherry* as a template, and the PCR product was used to replace the YFP fragment of *p413TEF-NYFP* and *p413TEF-NQYFP* after digestion with *XmaI* and *XhoI*, generating *p413TEF-NmCherry* and *p413TEF-NQmCherry*, respectively. Further, *NmCherry* and *NQmCherry* from *p413TEF-NmCherry* and *p413TEF-NQmCherry* were sub-cloned into *p423GAL1* through *Spe*I/*Xho*I sites, resulting in *p423GAL1-NmCherry* and *p423GAL1-NQmCherry*, respectively.

FLO11 promoter (P_{FLO11}) was PCR-amplified with primer pair of FLO11S-F/1-3R from template DNA extracted from LY746. To dissect the *FLO11* promoter, P_{F13} and P_{F16} were also PCR-amplified from LY746 genomic DNA using primer pairs of 1-3F/1-3R and 6F/1-3R, respectively. P_{F136} was generated by an overlapping PCR (bridge-PCR) – the primary PCR was done with primer pair of 6F/6R (with a 30-bp 3′ extension homologous to the 5′ sequence of P_{F13}, PCR 6) using the *FLO11* promoter PCR product as a template; and the secondary PCR was conducted with primer pair of 6F/1-3R using a mixture of PCR 6 and P_{F13} as template. P_{F1369} PCR product was also acquired by bridge-PCR – PCR was first

performed with primer pair of 9-10F/9-10R2 (with a 30-bp 3′ extension homologous to the 5′ sequence of PCR 6, PCR 9-10) using the *FLO11* promoter PCR product as a template followed by another round PCR that was carried out with primer pair of 9-10F/1-3R using PCR 9-10 and P_{F136} as templates. Similarly, PCR was done with a pair of primers,9-10F/9-10R1 (with a 30-bp 3′ extension homologous to the 5′ sequence of $P_{F13,}$ PCR 9-10a) using the full-length *FLO11* promoter PCR product as a template. Further, PCR using the primer pair of 9-10F/1-3R and PCR 9-10a and P_{F13} as templates created P_{F139}. The obtained PCR products of P_{FLO11}, P_{F13}, P_{F16}, P_{F136}, P_{F139}, P_{F1369} were then digested with *Xma*I and *Sac*II, and used to replace the *SUC2-LEU2* promoter in *p415SL-URA3*, leading to plasmids of *p415FLO11-URA3*, p415F13-URA3, p415F16-URA3, p415F136-URA3, p415F139-URA3, and *p415F1369-URA3*, respectively. Moreover, *ADH2* and *HO* promoters were PCR-amplified with primer pairs of ADH2-F/ADH2-R and HO-F/HO-R using the chromosomal DNA of YJW 426 as PCR template followed by another round of PCR using the first PCR products as templates, and the primer pairs of ADH2S-F/ADH2X-R and HOS-F/HOX-R. The resulting PCR products were then digested with *Xma*I and *Sac*II, and used to replace the *SUC2-LEU2* promoter in *p415SL-URA3* to generate *p415ADH2-URA3* and *p415HO-URA3*, respectively. Plasmid *p425GPD-SSE1* was constructed by sub-cloning *SSE1* from *p426GPD-SSE1* into *p425GPD* at the *Xho*I and *Spe*I sites. All the newly created plasmids were confirmed by restriction digestion and DNA sequencing.

Yeast Strain engineering and cultivation

DY902 was acquired by growing LY746 on media containing 5 mM GdnHCl to cure [PIN^+]. A successful curing was verified by lack of Rnq1-GFP aggregation upon transformation of the plasmid *pCUP1-RNQ1GFP*. Plasmid *pCUP1-RNQ1GFP* was then removed by counter selection on media containing 5-FOA. To replace the endogenous P_{FLO11}-*FLO11* with P_{F139}-*URA3*, P_{F139}-*URA3* fragment was firstly PCR-amplified with primers of Flo11ex-F and Flo11URA3-R using *p415F139-URA3* as template. The acquired PCR product was used as template for a secondary PCR with primer pair of Flo11ex-F/Flo11ex-R. The generated PCR product was then used to transform DY902, a wild-type non-prion BY4741 strain. The obtained Ura^+ isolates are potential gene replacement mutants which are further verified by PCR with primers of Flo11ex-F and Flo11ex-R, leading to BY4741 *flo8 flo11Δ:: P_{F139}-URA3* (DY767). DY767 was repaired for *FLO8* gene by introducing *Sal*I-digested *pRS303-FLO8* into the strain to create the strain DY759. A successful *FLO8* repair was indicated by a phenotypic switch from Adh^- (adhesion negative) His^- Ura^- to Adh^+ His^+ Ura^+. [SWI^+] was introduced into DY767 and DY759 by protein extract transformation as described later, leading to strains *flo8 flo11Δ:: P_{F139}-URA3* [SWI^+] (LY740) and *flo8::FLO8::HIS3 flo11Δ:: P_{F139}-URA3* [SWI^+] (LY744).

General yeast cultivation was performed as described previously (Fan *et al.*, 2007, Park *et al.*, 2006). LB, YPD, and SC (complete synthetic) media with certain amino acids dropout were used in this study otherwise specified. SC+5-FOA is a SC medium containing 0.1% 5-FOA, pH4.0. SC+raffinose+antimycin A has been previously described (Du *et al.*, 2008). In galactose induction experiments, 2% sucrose was used as the carbon source. To induce the expression of a *CUP1* promoter-controlled Sup35 NMGFP or Rnq1-GFP for examining their prion states, 50 μM $CuSO_4$ was usually supplemented into a medium otherwise 10 μM

$CuSO_4$ was used to study the interaction of Sup35, Rnq1 and Rnq1 at their prion initiation stage. For *Escherichia coli* cultures, 100 μg/ml ampicillin, or 30 mg/ml kanamycin was typically supplemented.

[SWI$^+$] transfer and PCR experiments

A protein extract transformation-based protocol for [*SWI*$^+$] transfer was described previously (Du *et al.*, 2010) with minimal modifications (Tanaka & Weissman, 2006). In this study, DY902 (with a chromosomal *TEF1-RNQ1-CFP* fusion gene) was used as a [*SWI*$^+$] donor because the Rnq1 prion status can be conveniently monitored. In the prion transfer experiment, plasmid *p415TEF-NQYFP* was also co-transformed into the recipient strain to facilitate a successful selection of [*SWI*$^+$]. A successful transfer of [*SWI*$^+$] was verified by Swi1 NQ-YFP aggregation and Raf$^{\pm}$ that were curable by 5 mM GdnHCl.

In this study, PrimeSTAR HS DNA Polymerase (TaKaRa) was used in PCR to amplify DNA for cloning purposes. To extract DNA from yeast cells for PCR, yeast cells from cultures or colonies were simply boiled for 10 min in 20 mM NaOH, briefly cleared by centrifugation at 600 g for 2 min, and the crude supernatants used as PCR templates.

Adhesive growth and flocculation assays

Adhesive growth on SC plates was performed as described previously (Braus *et al.*, 2003, Fichtner *et al.*, 2007, Roberts & Fink, 1994) with minor modifications. In brief, fresh cells were streaked or spread on proper SC selective plates, incubated for 3 days at 30°C and shifted to room temperature for additional 3 days before performing the washing assay. The washing assay was performed in a water bowl by swirling the plate for different times before taking images. A vigorous wash was done using tap water with or without rubbing.

Flocculation assay was carried our similarly to that reported before (Kobayashi *et al.*, 1996). Basically, after 2-3 days of growth in SC media, flocculating ability of cells was assessed based on appearance of visible cell aggregates. Saturated cell cultures were vigorously vortexed and images were taken as controls. Then images were taken in a time course to see appearance of cell pellets at the bottom of the tubes.

Fluorescence microscopy assays

In this study, GFP, YFP, CFP, and mCherry serve as fluorescence tags for various fusion proteins. These fluorescent proteins were either expressed ectopically from a plasmid or endogenously from a chromosomal tag. Methods for fluorescence microscopy were described previously [34]. For a constitutive promoter-driven expression, fresh colonies or log-phase cultures were used for microscopic observations. With an inducible promoter such as *CUP1* or *GAL1*, $CuSO_4$ or galactose was added in log-phase cultures to induce the expression of a fluorescent protein. In this study, a concentration gradient was tested in a time course for both kinds of inducers to determine their minimal concentrations in liquid media and/or on solid plates. For instance, 10 μM $CuSO_4$ was used as a minimal concentration for Sup35 NM-GFP and Rnq1-GFP expression to ensure visibility of their aggregation in [*PSI*$^+$] and [*PIN*$^+$] cells but to avoid unnecessary overproduction of the protein, respectively. Similarly, 0.02% of galactose in a sucrose-based medium was used as

minimum to detect Swi1 aggregation in cells without unnecessary overproduction for *GAL1* promoter.

Assays for [SWI$^+$] propagation and stability impacted by chaperone activities

A 74D-694 strain (LY722) or a BY4741 [*SWI*$^+$] strain (LY742) was co-transformed with *p415F139-URA3* and *p423GPD-SSE1* or *p2HGHSP104* to overproduce Sse1 or Hsp104, or *p423GPD* as an empty vector control. Transformants were grown for 24, 48 or 72 h in liquid culture then spread onto SC selective plates. Colonies were then replica-plated onto SC, SC +5-FOA and SC-uracil to test the status of [*SWI*$^+$]; and their prion state was further verified by assaying their raffinose-ultilyzing ability and aggregation of Swi1-NQYFP. Curing frequencies were normalized by total colony numbers obtained on SC plates. To see the effect of Hsp104 functional knock down by GdnHCl, the vector-transformed prion strains (with *p415F139-URA3*) were cultured in SC+5 mM GdnHCl medium in parallel before spreading and replica-plating experiments as described above. Swi1 N-YFP aggregation was also assayed for randomly picked colonies from SC plates after the phenotypic curing tests upon removing the reporter plasmid and reintroducing *p416TEF-NYFP.* Similar assays were performed with another BY4741 strain (LY735) carrying chromosomal reporter of P_{FLO1}-*URA3.* In addition, to see how overproduction of Sse1 or Hsp104 affects [*SWI*$^+$]-curing by GdnHCl, LY735 carrying *p425GPD-SSE1*, *p425GPD-HSP104*, or *p425GPD* was cultured for 24, 48, and 72 h in 5 mM GdnHCl-containing SC selective medium, and assayed for stability of [*SWI*$^+$] similarly.

[SWI$^+$] de novo formation assays

To assay spontaneous [*SWI*$^+$] conversion frequency in BY4741 cells, a non-prion *flo8::FLO8::HIS3 flo1::*P_{FLo1}*-URA3* strain (LY735) was cultured overnight in liquid YPD until reaching the stationary phase and spread onto SC-his and SC-his+5-FOA plates after proper dilution. Colonies that appeared on the 5-FOA plates were treated at least twice on SC-his+5 mM GdnHCl before replica-plating back to SC-his plates without uracil and SC-his+5-FOA plates to check their curability. Curable isolates were then transformed with *p415TEF-NQYFP* for aggregation assay to confirm the [*SWI*$^+$] prion status. For 74D-694 strains, isogenic [*PSI*$^+$], [*PIN*$^+$], and non-prion strains carrying the reporter plasmid *p415F139-URA3* and *p413GAL1-NQYFP* were cultured in SC-leu for 2 days until the stationary phase before spreading onto SC-leu and SC-leu + 5-FOA plates after proper dilution. Colonies that appeared on 5-FOA plates were replica-plated twice onto the same plates to stabilize the prion conformations before replica-plating onto SC-leu-his sucrose plates supplemented with 0.02% galactose to verify the presence of [*SWI*$^+$] prion by NQ-YFP aggregation assay. Isolates with at least more than 30% cells containing NQ-YFP aggregates were further colony-purified and assayed again. Eventually, isolates with at least 60% of cells containing NQ-YFP aggregation were scored as [*SWI*$^+$] isolates. To assay Swi1 PrD-promoted [*SWI*$^+$] formation, 74D-694 strains with different prion backgrounds Swi1-NYFP were co-transformed with *p423GAL1-NYFP* and *p415F139-URA3.* Sucrose-based log-phase cultures were then supplemented with or without 0.5% galactose and induced for 24 h before spreading onto SC-leu-his and SC-leu-his+5-FOA plates. 5-FOA$^+$ isolates were then tested for the aggregation of NYFP on 0.02% galactose sucrose plates to verify their prion status as aforementioned. Aggregation and prion phenotypes were then verified by

their curability by GdnHCl. In all these experiments, [*SWI*$^{+}$] rates were normalized with the total cells achieved on SC plates.

Supplementary Material

Refer to Web version on PubMed Central for supplementary material.

Acknowledgments

The authors thank Drs. S. Lindquist (Whitehead Institute for Biomedical Research, Department of Biology, Massachusetts Institute of Technology and Howard Hughes Medical Institute, and G. Braus (Georg August University Göttingen, Institute for Microbiology and Genetics) for providing us plasmids, strains, and other experimental materials. This work was supported by grants from the U.S. National Institutes of Health (R01GM110045) and U.S. National Science Foundation (MCB 1122135) to LL.

References

Aguzzi A, O'Connor T. Protein aggregation diseases: pathogenicity and therapeutic perspectives. Nature reviews. Drug discovery. 2010; 9:237–248. [PubMed: 20190788]

Aigle M, Lacroute F. Genetical aspects of [URE3], a non-mitochondrial, cytoplasmically inherited mutation in yeast. Molecular & general genetics : MGG. 1975; 136:327–335. [PubMed: 16095000]

Alberti S, Halfmann R, King O, Kapila A, Lindquist S. A systematic survey identifies prions and illuminates sequence features of prionogenic proteins. Cell. 2009; 137:146–158. [PubMed: 19345193]

Alonso A, Zaidi T, Novak M, Grundke-Iqbal I, Iqbal K. Hyperphosphorylation induces self-assembly of tau into tangles of paired helical filaments/straight filaments. Proceedings of the National Academy of Sciences of the United States of America. 2001; 98:6923–6928. [PubMed: 11381127]

Ano Bom AP, Rangel LP, Costa DC, de Oliveira GA, Sanches D, Braga CA, Gava LM, Ramos CH, Cepeda AO, Stumbo AC, De Moura Gallo CV, Cordeiro Y, Silva JL. Mutant p53 aggregates into prion-like amyloid oligomers and fibrils: implications for cancer. The Journal of biological chemistry. 2012; 287:28152–28162. [PubMed: 22715097]

Bagriantsev S, Liebman SW. Specificity of prion assembly in vivo. [PSI+] and [PIN+] form separate structures in yeast. The Journal of biological chemistry. 2004; 279:51042–51048. [PubMed: 15465809]

Barrales RR, Jimenez J, Ibeas JI. Identification of novel activation mechanisms for FLO11 regulation in Saccharomyces cerevisiae. Genetics. 2008; 178:145–156. [PubMed: 18202364]

Barrales RR, Korber P, Jimenez J, Ibeas JI. Chromatin modulation at the FLO11 promoter of Saccharomyces cerevisiae by HDAC and Swi/Snf complexes. Genetics. 2012; 191:791–803. [PubMed: 22542969]

Basu U, Southron JL, Stephens JL, Taylor GJ. Reverse genetic analysis of the glutathione metabolic pathway suggests a novel role of PHGPX and URE2 genes in aluminum resistance in Saccharomyces cerevisiae. Mol Genet Genomics. 2004; 271:627–637. [PubMed: 15133656]

Bester MC, Pretorius IS, Bauer FF. The regulation of Saccharomyces cerevisiae FLO gene expression and Ca2+ -dependent flocculation by Flo8p and Mss11p. Current genetics. 2006; 49:375–383. [PubMed: 16568252]

Biddick RK, Law GL, Chin KK, Young ET. The transcriptional coactivators SAGA, SWI/SNF, and mediator make distinct contributions to activation of glucose-repressed genes. The Journal of biological chemistry. 2008; 283:33101–33109. [PubMed: 18826948]

Brachmann A, Toombs JA, Ross ED. Reporter assay systems for [URE3] detection and analysis. Methods. 2006

Bradley ME, Edskes HK, Hong JY, Wickner RB, Liebman SW. Interactions among prions and prion "strains" in yeast. Proceedings of the National Academy of Sciences of the United States of America. 2002; 99(Suppl 4):16392–16399. [PubMed: 12149514]

Braus GH, Grundmann O, Bruckner S, Mosch HU. Amino acid starvation and Gcn4p regulate adhesive growth and FLO11 gene expression in Saccharomyces cerevisiae. Molecular biology of the cell. 2003; 14:4272–4284. [PubMed: 14517335]

Chakrabortee S, Byers JS, Jones S, Garcia DM, Bhullar B, Chang A, She R, Lee L, Fremin B, Lindquist S, Jarosz DF. Intrinsically Disordered Proteins Drive Emergence and Inheritance of Biological Traits. Cell. 2016; 167:369–381. e312. [PubMed: 27693355]

Chernoff YO, Lindquist SL, Ono B, Inge-Vechtomov SG, Liebman SW. Role of the chaperone protein Hsp104 in propagation of the yeast prion-like factor [PSI^+]. Science. 1995; 268:880–884. [PubMed: 7754373]

Chiti F, Dobson CM. Protein misfolding, functional amyloid, and human disease. Annual review of biochemistry. 2006; 75:333–366.

Colby DW, Prusiner SB. Prions. Cold Spring Harb Perspect Biol. 2011; 3:a006833. [PubMed: 21421910]

Crow ET, Li L. Newly identified prions in budding yeast, and their possible functions. Seminars in cell & developmental biology. 2011; 22:452–459. [PubMed: 21397710]

Derkatch IL, Bradley ME, Hong JY, Liebman SW. Prions affect the appearance of other prions: the story of [PIN^+]. Cell. 2001; 106:171–182. [PubMed: 11511345]

Derkatch IL, Bradley ME, Zhou P, Chernoff YO, Liebman SW. Genetic and environmental factors affecting the de novo appearance of the [PSI^+] prion in Saccharomyces cerevisiae. Genetics. 1997; 147:507–519. [PubMed: 9335589]

Derkatch IL, Uptain SM, Outeiro TF, Krishnan R, Lindquist SL, Liebman SW. Effects of Q/N-rich, polyQ, and non-polyQ amyloids on the de novo formation of the [PSI+] prion in yeast and aggregation of Sup35 in vitro. Proceedings of the National Academy of Sciences of the United States of America. 2004; 101:12934–12939. [PubMed: 15326312]

Du Z, Crow ET, Kang HS, Li L. Distinct subregions of Swi1 manifest striking differences in prion transmission and SWI/SNF function. Molecular and cellular biology. 2010; 30:4644–4655. [PubMed: 20679490]

Du Z, Li L. Investigating the interactions of yeast prions: [SWI+], [PSI+], and [PIN+]. Genetics. 2014; 197:685–700. [PubMed: 24727082]

Du Z, Park KW, Yu H, Fan Q, Li L. Newly identified prion linked to the chromatin-remodeling factor Swi1 in Saccharomyces cerevisiae. Nat Genet. 2008; 40:460–465. [PubMed: 18362884]

Du Z, Valtierra S, Li L. An insight into the complex prion-prion interaction network in the budding yeast Saccharomyces cerevisiae. Prion. 2014; 8:387–392. [PubMed: 25517561]

Du Z, Zhang Y, Li L. The Yeast Prion [SWI(+)] Abolishes Multicellular Growth by Triggering Conformational Changes of Multiple Regulators Required for Flocculin Gene Expression. Cell reports. 2015; 13:2865–2878. [PubMed: 26711350]

Eisenberg D, Jucker M. The amyloid state of proteins in human diseases. Cell. 2012; 148:1188–1203. [PubMed: 22424229]

Fan Q, Park KW, Du Z, Morano KA, Li L. The role of Sse1 in the de novo formation and variant determination of the [PSI+] prion. Genetics. 2007; 177:1583–1593. [PubMed: 18039878]

Fichtner L, Schulze F, Braus GH. Differential Flo8p-dependent regulation of FLO1 and FLO11 for cell-cell and cell-substrate adherence of S. cerevisiae S288c. Molecular microbiology. 2007; 66:1276–1289. [PubMed: 18001350]

Fleming AB, Pennings S. Antagonistic remodelling by Swi-Snf and Tup1-Ssn6 of an extensive chromatin region forms the background for FLO1 gene regulation. The EMBO journal. 2001; 20:5219–5231. [PubMed: 11566885]

Gotz J, Chen F, van Dorpe J, Nitsch RM. Formation of neurofibrillary tangles in P301l tau transgenic mice induced by Abeta 42 fibrils. Science. 2001; 293:1491–1495. [PubMed: 11520988]

Guinan E, Jones GW. Influence of Hsp70 chaperone machinery on yeast prion propagation. Protein Pept Lett. 2009; 16:583–586. [PubMed: 19519515]

Guo JL, Covell DJ, Daniels JP, Iba M, Stieber A, Zhang B, Riddle DM, Kwong LK, Xu Y, Trojanowski JQ, Lee VM. Distinct alpha-synuclein strains differentially promote tau inclusions in neurons. Cell. 2013; 154:103–117. [PubMed: 23827677]

Halfmann R, Wright JR, Alberti S, Lindquist S, Rexach M. Prion formation by a yeast GLFG nucleoporin. Prion. 2012; 6:391–399. [PubMed: 22561191]

Hines JK, Craig EA. The sensitive [SWI (+)] prion: new perspectives on yeast prion diversity. Prion. 2011; 5:164–168. [PubMed: 21811098]

Hines JK, Li X, Du Z, Higurashi T, Li L, Craig EA. [SWI], the prion formed by the chromatin remodeling factor Swi1, is highly sensitive to alterations in Hsp70 chaperone system activity. PLoS genetics. 2011; 7:e1001309. [PubMed: 21379326]

Holmes DL, Lancaster AK, Lindquist S, Halfmann R. Heritable remodeling of yeast multicellularity by an environmentally responsive prion. Cell. 2013; 153:153–165. [PubMed: 23540696]

Huang VJ, Stein KC, True HL. Spontaneous variants of the [RNQ+] prion in yeast demonstrate the extensive conformational diversity possible with prion proteins. PloS one. 2013; 8:e79582. [PubMed: 24205387]

Jarosz DF, Lancaster AK, Brown JC, Lindquist S. An evolutionarily conserved prion-like element converts wild fungi from metabolic specialists to generalists. Cell. 2014; 158:1072–1082. [PubMed: 25171408]

Kabani M, Beckerich JM, Brodsky JL. Nucleotide exchange factor for the yeast Hsp70 molecular chaperone Ssa1p. Molecular and cellular biology. 2002; 22:4677–4689. [PubMed: 12052876]

Kawai-Noma S, Pack CG, Kojidani T, Asakawa H, Hiraoka Y, Kinjo M, Haraguchi T, Taguchi H, Hirata A. In vivo evidence for the fibrillar structures of Sup35 prions in yeast cells. The Journal of cell biology. 2010; 190:223–231. [PubMed: 20643880]

Kim HY, Lee SB, Kang HS, Oh GT, Kim T. Two distinct domains of Flo8 activator mediates its role in transcriptional activation and the physical interaction with Mss11. Biochemical and biophysical research communications. 2014; 449:202–207. [PubMed: 24813990]

King OD, Gitler AD, Shorter J. The tip of the iceberg: RNA-binding proteins with prion-like domains in neurodegenerative disease. Brain research. 2012; 1462:61–80. [PubMed: 22445064]

Kobayashi O, Suda H, Ohtani T, Sone H. Molecular cloning and analysis of the dominant flocculation gene FLO8 from Saccharomyces cerevisiae. Molecular & general genetics : MGG. 1996; 251:707–715. [PubMed: 8757402]

Kobayashi O, Yoshimoto H, Sone H. Analysis of the genes activated by the FLO8 gene in Saccharomyces cerevisiae. Current genetics. 1999; 36:256–261. [PubMed: 10591965]

Kryndushkin D, Wickner RB. Nucleotide exchange factors for Hsp70s are required for [URE3] prion propagation in Saccharomyces cerevisiae. Molecular biology of the cell. 2007; 18:2149–2154. [PubMed: 17392510]

Lancaster AK, Bardill JP, True HL, Masel J. The spontaneous appearance rate of the yeast prion [PSI +] and its implications for the evolution of the evolvability properties of the [PSI+] system. Genetics. 2010; 184:393–400. [PubMed: 19917766]

Landreh M, Sawaya MR, Hipp MS, Eisenberg DS, Wuthrich K, Hartl FU. The formation, function and regulation of amyloids: insights from structural biology. J Intern Med. 2016

Li F, Palecek SP. Identification of Candida albicans genes that induce Saccharomyces cerevisiae cell adhesion and morphogenesis. Biotechnology progress. 2005; 21:1601–1609. [PubMed: 16321041]

Liu H, Styles CA, Fink GR. Saccharomyces cerevisiae S288C has a mutation in FLO8, a gene required for filamentous growth. Genetics. 1996; 144:967–978. [PubMed: 8913742]

Luk KC, Kehm V, Carroll J, Zhang B, O'Brien P, Trojanowski JQ, Lee VM. Pathological alpha-synuclein transmission initiates Parkinson-like neurodegeneration in nontransgenic mice. Science. 2012; 338:949–953. [PubMed: 23161999]

Mao X, Li Y, Wang H, Cao F, Chen J. Antagonistic interplay of Swi1 and Tup1 on filamentous growth of Candida albicans. FEMS microbiology letters. 2008; 285:233–241. [PubMed: 18564337]

Masison DC, Reidy M. Yeast prions are useful for studying protein chaperones and protein quality control. Prion. 2015; 9:174–183. [PubMed: 26110609]

Mathur V, Taneja V, Sun Y, Liebman SW. Analyzing the birth and propagation of two distinct prions, [PSI+] and [Het-s](y), in yeast. Molecular biology of the cell. 2010; 21:1449–1461. [PubMed: 20219972]

Mayhew D, Mitra RD. Transcription factor regulation and chromosome dynamics during pseudohyphal growth. Molecular biology of the cell. 2014; 25:2669–2676. [PubMed: 25009286]

Mukai H, Kuno T, Tanaka H, Hirata D, Miyakawa T, Tanaka C. Isolation and characterization of SSE1 and SSE2, new members of the yeast HSP70 multigene family. Gene. 1993; 132:57–66. [PubMed: 8406043]

Munch C, O'Brien J, Bertolotti A. Prion-like propagation of mutant superoxide dismutase-1 misfolding in neuronal cells. Proceedings of the National Academy of Sciences of the United States of America. 2011; 108:3548–3553. [PubMed: 21321227]

Neigeborn L, Carlson M. Mutations causing constitutive invertase synthesis in yeast: genetic interactions with snf mutations. Genetics. 1987; 115:247–253. [PubMed: 3549450]

Ono K, Takahashi R, Ikeda T, Yamada M. Cross-seeding effects of amyloid beta-protein and alpha-synuclein. Journal of neurochemistry. 2012; 122:883–890. [PubMed: 22734715]

Osherovich LZ, Weissman JS. Multiple Gln/Asn-rich prion domains confer susceptibility to induction of the yeast [PSI^{+}] prion. Cell. 2001; 106:183–194. [PubMed: 11511346]

Park KW, Hahn JS, Fan Q, Thiele DJ, Li L. De Novo Appearance and "Strain" Formation of Yeast Prion [PSI+] Are Regulated by the Heat-Shock Transcription Factor. Genetics. 2006; 173:35–47. [PubMed: 16452152]

Patino MM, Liu JJ, Glover JR, Lindquist S. Support for the prion hypothesis for inheritance of a phenotypic trait in yeast. Science. 1996; 273:622–626. [PubMed: 8662547]

Prusiner SB. Novel proteinaceous infectious particles cause scrapie. Science. 1982; 216:136–144. [PubMed: 6801762]

Prusiner SB. Prions. Proceedings of the National Academy of Sciences of the United States of America. 1998; 95:13363–13383. [PubMed: 9811807]

Prusiner SB. Cell biology. A unifying role for prions in neurodegenerative diseases. Science. 2012; 336:1511–1513. [PubMed: 22723400]

Roberts RL, Fink GR. Elements of a single MAP kinase cascade in Saccharomyces cerevisiae mediate two developmental programs in the same cell type: mating and invasive growth. Genes & development. 1994; 8:2974–2985. [PubMed: 8001818]

Rogoza T, Goginashvili A, Rodionova S, Ivanov M, Viktorovskaya O, Rubel A, Volkov K, Mironova L. Non-Mendelian determinant [ISP+] in yeast is a nuclear-residing prion form of the global transcriptional regulator Sfp1. Proceedings of the National Academy of Sciences of the United States of America. 2010; 107:10573–10577. [PubMed: 20498075]

Romanova NV, Chernoff YO. Hsp104 and prion propagation. Protein Pept Lett. 2009; 16:598–605. [PubMed: 19519517]

Rupp S, Summers E, Lo HJ, Madhani H, Fink G. MAP kinase and cAMP filamentation signaling pathways converge on the unusually large promoter of the yeast FLO11 gene. The EMBO journal. 1999; 18:1257–1269. [PubMed: 10064592]

Sanders DW, Kaufman SK, DeVos SL, Sharma AM, Mirbaha H, Li A, Barker SJ, Foley AC, Thorpe JR, Serpell LC, Miller TM, Grinberg LT, Seeley WW, Diamond MI. Distinct tau prion strains propagate in cells and mice and define different tauopathies. Neuron. 2014; 82:1271–1288. [PubMed: 24857020]

Schwimmer C, Masison DC. Antagonistic interactions between yeast [PSI(+)] and [URE3] prions and curing of [URE3] by Hsp70 protein chaperone Ssa1p but not by Ssa2p. Molecular and cellular biology. 2002; 22:3590–3598. [PubMed: 11997496]

Serio TR, Lindquist SL. [PSI^{+}]: an epigenetic modulator of translation termination efficiency. Annual review of cell and developmental biology. 1999; 15:661–703.

Sondheimer N, Lindquist S. Rnq1: an epigenetic modifier of protein function in yeast. Molecular cell. 2000; 5:163–172. [PubMed: 10678178]

Soto C. Unfolding the role of protein misfolding in neurodegenerative diseases. Nat Rev Neurosci. 2003; 4:49–60. [PubMed: 12511861]

Soto C. Transmissible proteins: expanding the prion heresy. Cell. 2012; 149:968–977. [PubMed: 22632966]

Spillantini MG, Schmidt ML, Lee VM, Trojanowski JQ, Jakes R, Goedert M. Alpha-synuclein in Lewy bodies. Nature. 1997; 388:839–840. [PubMed: 9278044]

Sporn ZA, Hines JK. Hsp40 function in yeast prion propagation: Amyloid diversity necessitates chaperone functional complexity. Prion. 2015; 9:80–89. [PubMed: 25738774]

Stansfield I, Jones KM, Kushnirov VV, Dagkesamanskaya AR, Poznyakovski AI, Paushkin SV, Nierras CR, Cox BS, Ter-Avanesyan MD, Tuite MF. The products of the SUP45 (eRF1) and SUP35 genes interact to mediate translation termination in Saccharomyces cerevisiae. The EMBO journal. 1995; 14:4365–4373. [PubMed: 7556078]

Stein KC, True HL. Prion strains and amyloid polymorphism influence phenotypic variation. PLoS pathogens. 2014; 10:e1004328. [PubMed: 25188330]

Stern M, Jensen R, Herskowitz I. Five SWI genes are required for expression of the HO gene in yeast. Journal of molecular biology. 1984; 178:853–868. [PubMed: 6436497]

Suzuki G, Shimazu N, Tanaka M. A yeast prion, Mod5, promotes acquired drug resistance and cell survival under environmental stress. Science. 2012; 336:355–359. [PubMed: 22517861]

Tanaka M, Weissman JS. An efficient protein transformation protocol for introducing prions into yeast. Methods Enzymol. 2006; 412:185–200. [PubMed: 17046659]

Tyedmers J, Madariaga ML, Lindquist S. Prion switching in response to environmental stress. PLoS biology. 2008; 6:e294. [PubMed: 19067491]

Tyedmers J, Treusch S, Dong J, McCaffery JM, Bevis B, Lindquist S. Prion induction involves an ancient system for the sequestration of aggregated proteins and heritable changes in prion fragmentation. Proceedings of the National Academy of Sciences of the United States of America. 2010; 107:8633–8638. [PubMed: 20421488]

Vassar R, Bennett BD, Babu-Khan S, Kahn S, Mendiaz EA, Denis P, Teplow DB, Ross S, Amarante P, Loeloff R, Luo Y, Fisher S, Fuller J, Edenson S, Lile J, Jarosinski MA, Biere AL, Curran E, Burgess T, Louis JC, Collins F, Treanor J, Rogers G, Citron M. Beta-secretase cleavage of Alzheimer's amyloid precursor protein by the transmembrane aspartic protease BACE. Science. 1999; 286:735–741. [PubMed: 10531052]

Volkov KV, Aksenova AY, Soom MJ, Osipov KV, Svitin AV, Kurischko C, Shkundina IS, Ter-Avanesyan MD, Inge-Vechtomov SG, Mironova LN. Novel non-Mendelian determinant involved in the control of translation accuracy in Saccharomyces cerevisiae. Genetics. 2002; 160:25–36. [PubMed: 11805042]

Wickner RB. [URE3] as an altered Ure2 protein: evidence for a prion analog in Saccharomyces cerevisiae. Science. 1994; 264:566–569. [PubMed: 7909170]

Wickner RB, Edskes HK, Bateman DA, Gorkovskiy A, Dayani Y, Bezsonov EE, Mukhamedova M. Yeast prions: proteins templating conformation and an anti-prion system. PLoS pathogens. 2015; 11:e1004584. [PubMed: 25654539]

Winkler J, Tyedmers J, Bukau B, Mogk A. Chaperone networks in protein disaggregation and prion propagation. Journal of structural biology. 2012; 179:152–160. [PubMed: 22580344]

Zhou P, Derkatch IL, Liebman SW. The relationship between visible intracellular aggregates that appear after overexpression of Sup35 and the yeast prion-like elements [PSI^+] and [PIN^+]. Molecular microbiology. 2001; 39:37–46. [PubMed: 11123686]

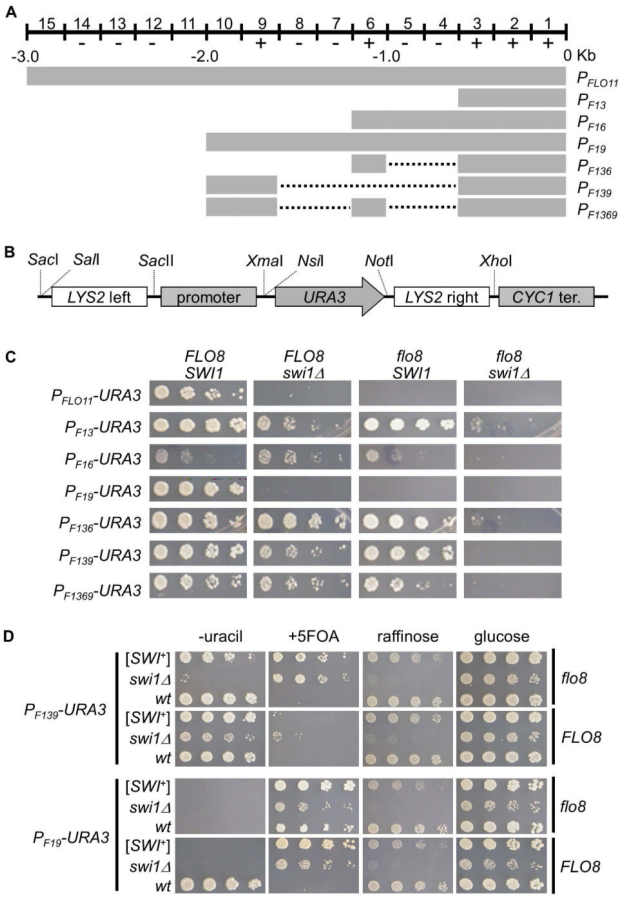

Figure 1. Dissection of *FLO11* promoter and construction of plasmid-based [*SWI*$^+$] reporters for S288C strains

(**A**) A diagrammatic illustration of the wild-type and truncation mutant *FLO11* promoters. The 3-kb *FLO11* promoter (P_{FLO11}) spans 15 0.2-kb segments carrying 7 upstream repression sequences (URSs, −) and 5 upstream activation sequences (UASs, +). The dotted lines stand for regions that are deleted. Construction strategies are shown in Figure S1. (**B**) A diagram showing the structure of constructed reporter plasmids. *URA3* gene serves as a reporter gene driven the wild type or a truncated *FLO11* promoter shown in A. *CYC1* terminator was included for all the constructs. 50-bp upstream and downstream extensions of *LYS2* flank the reporter to provide an option to integrate a reporter into chromosome. (**C**) BY4741 non-prion strains with the indicated genotypes were transformed with individual *p415*-based *URA3* reporter plasmids. Cells were spotted onto synthetic complete (SC) selective plates without uracil. Images were taken 3 days post spotting. Shown is a representative result of at least three independent experiments. (**D**) The indicated *FLO8* or *flo8* strains with distinct Swi1 status were transformed with either P_{F139}-*URA3* or P_{F19}-*URA3* plasmid and assayed for growth on glucose-containing SC medium (glucose) without uracil (−uracil), or with 5-FOA (+5FOA). Raffinose plate (glucose-free) was also included to verify the Swi1 status. Shown are representative results (3 days post-spotting) of at least three repeated tests.

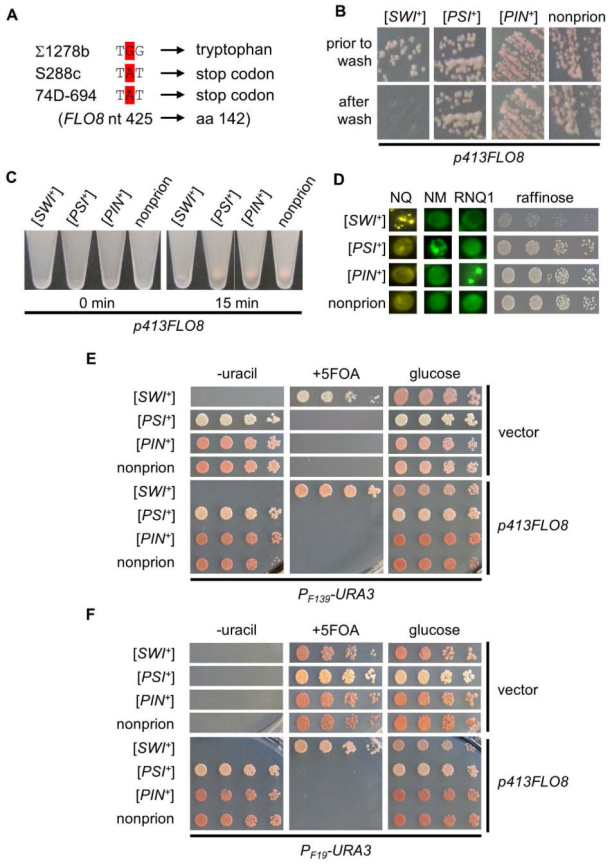

Figure 2. Performance of P_{F139}-*URA3* and P_{F19}-*URA3* plasmids as [*SWI*$^+$] reporters for 74D-694 derivatives

(**A**) DNA sequencing data demonstrate that the 74D-694 strain contains the same nonsense mutation in the *FLO8* ORF as S288C-derived strains. (**B**) Plasmid *p413FLO8* was introduced into the four indicated strains to ectopically express Flo8 under its own promoter. Transformants were then tested for adhesion on SC selective plates using a wash assay (see Experimental Procedures). The remaining cells were imaged prior to and after washing (a representative result of at least three repeated assays). (**C**) The same strains used in panel B were assayed for flocculation (cell-cell adhesion, or cell aggregation, see details in Experimental Procedures). 0 min, immediately after vortexing the cell cultures; 15 min, 15 min after keeping cultures still on bench post-vortex. Shown is a typical result of at least three repeated tests. (**D**) Indicated isogenic 74D-694 strains were examined for raffinose phenotype (right) and aggregation patterns of Swi1-NQ-YFP (NQ), Sup35-NM-GFP (NM) and Rnq1-GFP (RNQ1) after transforming them with *p416TEF-NQYFP*, *pCUP1-NMGFP*, or *pCUP1-RNQ1GFP*. (**E**) Indicated strains were co-transformed with *p415F139-URA3* and *p413FLO8* or *p413TEF* (vector), and assayed for their growth on glucose-containing SC medium (glucose) without uracil (−uracil), or with 5-FOA (+5FOA). Shown are representative results (3 days post-spotting) of at least three repeated assays. (**F**) Experiment was carried out similar to that in panel E except that *p415F19-URA3* was used instead of *p415F139-URA3.*

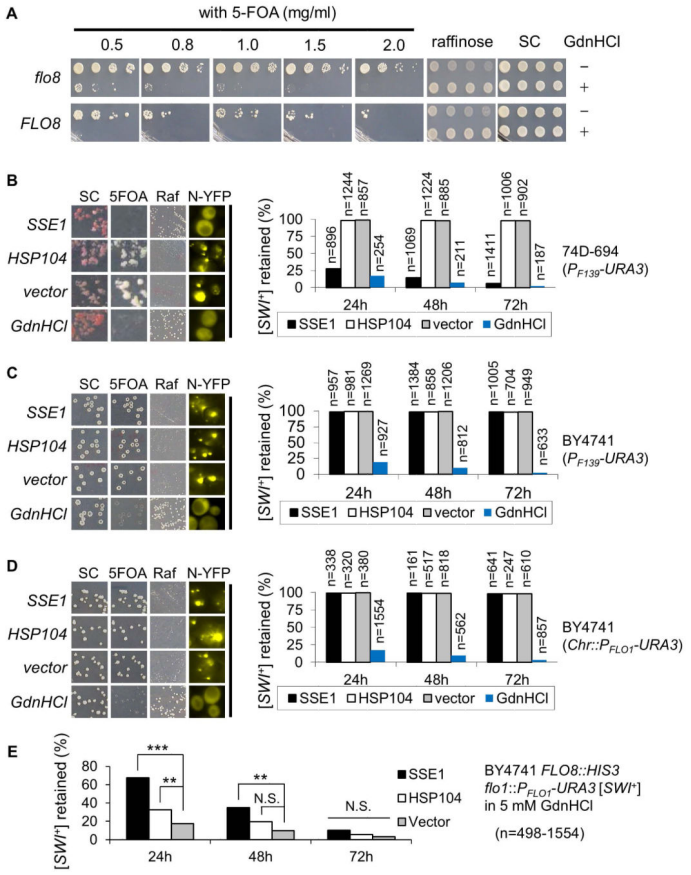

Figure 3. The effect of altering Hsp104 and Sse1 activity on [*SWI*$^+$] propagation

(**A**) *FLO8*-repaired (*FLO8*) and unrepaired (*flo8)* BY4741 [*SWI*$^+$] strains were transformed with *p415F139-URA3,* and streaked on SC selective plates (SC) with (+) or without (−) 5 mM GdnHCl and then cultured in SC-leu which was followed by growth on the indicated SC selective plates. Shown was a result (3 days post-spotting) of at least 3 independent experiments. (**B**, **C, and D**) As described in the Experimental Procedures, the influences of Hsp104 overproduction (*HSP104*), Hsp104 inactivation (*GdnHCl*), and Sse1 overproduction (*SSE1*) on [*SWI*$^+$] propagation in 74D-694 (**B**) and BY4741 (**C** and **D**) backgrounds were investigated. *vector*, an empty vector control; SC, SC selective plate; 5FOA, SC selective plate with 5-FOA; Raf, raffinose plate; n, total colonies assayed. Note: the plasmid reporter P_{F139}-*URA3* was used for panel B and C, but chromosomal reporter of P_{FLO1}-*URA3* for panel D. Prion curing was summarized in the plot (right panel) based on the growth phenotypes (left). (**E**) Effect of Sse1 or Hsp104 overproduction on [*SWI*$^+$] curing by GdnHCl was assayed as described in the Experimental Procedures. The remaining [*SWI*$^+$] was assayed after growing cells in SC+GdnHCl medium for the indicated time while overproducing Hsp104 or Sse1. T-test was used to estimate the significance of the differences (N.S., not significant; **, P<0.01; ***, P<0.001). n, colonies assayed.

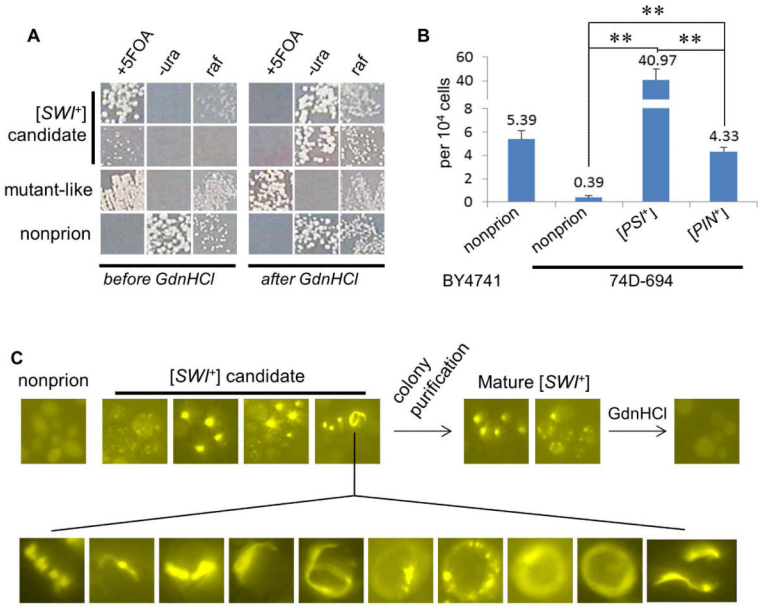

Figure 4. [*SWI*$^+$] spontaneous *de novo* formation promoted by pre-existing [*PSI*$^+$] or [*PIN*$^+$]

(**A**) Representative growth phenotypes of the BY4741 strain-derived [*SWI*$^+$] candidate isolates before and after 5 mM GdnHCl treatment. The [*SWI*$^+$] converting frequency is summarized in panel B. +5FOA (SC-his+5-FOA); −ura (SC-his-ura); raf (raffinose). (**B**) As described in the Experimental Procedures, [*SWI*$^+$] spontaneous conversion frequencies in the indicated strain backgrounds were summarized based on at least three independent experiments. (**C**) Appearance, maturation and curability of Swi1-NQ-YFP aggregation during Swi1 prionogenesis in 74D-694 strains. Upon colony purification, aggregation appeared in 5-FOA$^+$ cells could be stabilized, morphologically remodeled, and curable. Experiments were done for the [*PSI*$^+$], [*PIN*$^+$] and nonprion strains, and [*SWI*$^+$] converting frequencies are summarized in panel B. Shown here are representative data (upper, from non-prion strain; lower, ring/ribbon-like aggregates from [*PSI*$^+$] and [*PIN*$^+$] strains). Statistical analysis was performed by T test (**, P<0.01).

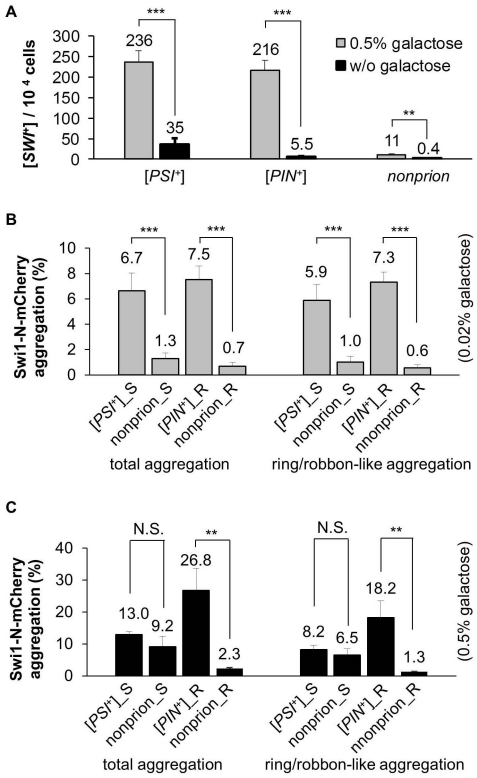

Figure 5. Aggregation and [*SWI*$^+$] *de novo* formation are promoted by overproduction of Swi1 PrD

(**A**) Overproduction of Swi1 PrD promotes [*SWI*$^+$] conversion. As described in the Experimental Procedures, with Swi1-NYFP overproduction (0.5% gal) or without (w/o gal), [*SWI*$^+$] frequencies were plotted for the indicated 74D-694 strains carrying the P_{F139}-*URA3* reporter plasmid. (**B** and **C**) The indicated three 74D-694 strains, [*PSI*$^+$], [*PIN*$^+$], and non-prion, were co-transformed with *p423GAL1-NmCherry* and *pCUP1-NMGFP* (for [*PSI*$^+$], [*PSI*$^+$]_S; and non-prion, nonprion_S), or with *p423GAL1-NmCherry* and *pCUP1-RNQ1GFP* (for [*PIN*$^+$], [*PIN*$^+$]_R and non-prion_R). SC-leu-ura sucrose cultures of the transformants were supplemented with 0.02% (**B**) or 0.5% (**C**) galactose and 10 μM $CuSO_4$. After incubation for 48 h, percentages of cells with all types of aggregation (total aggregation) or ring/ribbon-like only aggregation of Swi1-N-mCherry are shown. Statistical analysis for panel A-C was performed by T test (N.S, not significant; **, P<0.01; ***, P<0.001).

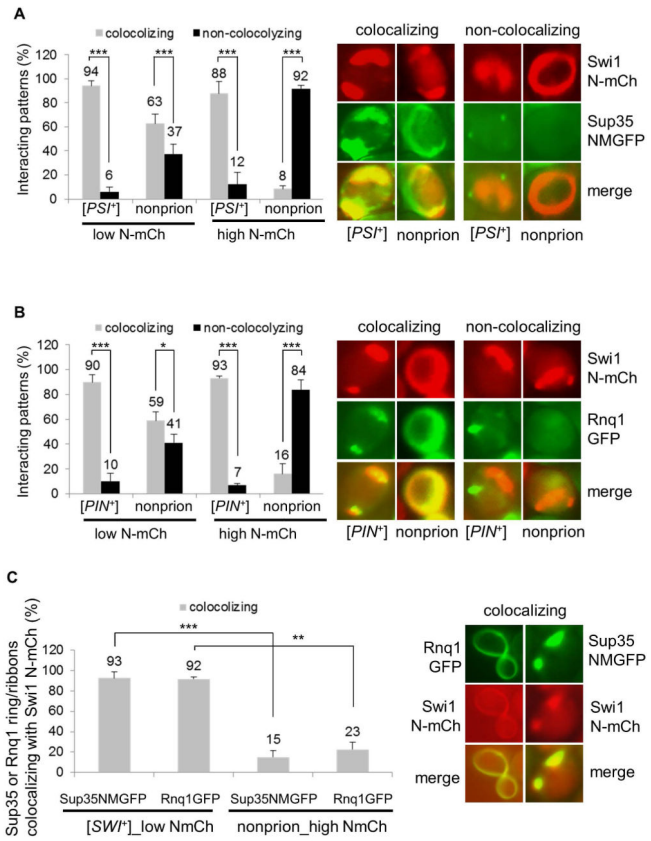

Figure 6. Interacting mechanisms of heterologous prion proteins, Sup35, Rnq1 and Swi1, in their prionogenesis

(**A**) The indicated 74D-694 strains were co-transformed with *p423GAL1-NmCherry* and *pCUP1-NMGFP*. The ring/ribbon-like Swi1 N-mCherry aggregates (NmCh) that are supposed to be prionogenic in Swi1 prionogenesis were quantified for their interaction with Sup35-NMGFP (NMGFP) at low (low N-mCh, 0.02% galactose) or high (high N-mCh, 0.5% galactose) production of Swi1 PrD. Notably, 10 μM $CuSO_4$ was supplemented, and both co-localizing and non-co-localizing patterns were observed after 48 h induction. The images shown on the right are representatives and plots are a summary of data from at least three independent experiments. (**B**) Similar to panel A, but the 74D-694 strains were co-transformed with *p423GAL1-NmCherry* and *pCUP1-NMGFP*, and the interaction is for Swi1 N-mCh and Rnq1-GFP. (**C**) A [*SWI*$^+$] or a non-prion 74D-694 strain was co-transformed with *p423GAL1-NmCherry* and *pCUP1-NMGFP*, or with *p423GAL1-NmCherry pCUP1-RNQ1GFP*. Subsequently, the newly formed Sup35 NM-GFP (NMGFP) and Rnq1-GFP ring/ribbon-like aggregates were assayed for colocalization with Swi1 N-mCherry after 48 h of incubation. Low NmCh, 0.02% galactose; high NmCh, 0.5% galactose. In the experiment, 10 μM $CuSO_4$ was supplied as minimum to visualize Sup35 NMGFP and Rnq1-GFP aggregation. Here shows a summary of the colocalizing frequencies (left) and representative images of the co-localization (right). Statistical analysis in the figure was performed by T test (*, P<0.05; **, P<0.01; ***, P<0.001).